Science of the Total Environment 717 (2020) 137047

Contents lists available at ScienceDirect

Science of the Total Environment

journal homepage: www.elsevier.com/locate/scitotenv

Terrestrial organic matter input drives sedimentary trace metal sequestration in a human-impacted boreal estuary

Sami A. Jokinen [a,b,*], Tom Jilbert [a,c], Rosa Tiihonen-Filppula [a], Karoliina Koho [a]

[a] Aquatic Biogeochemistry Research Unit, Ecosystems and Environment Research Program, Faculty of Biological and Environmental Sciences, University of Helsinki, P.O. Box 65, FI-00014 Helsinki, Finland
[b] Lake and Marine Sediment Research Group, Department of Geography and Geology, University of Turku, FI-20014 Turku, Finland
[c] Tvärminne Zoological Station, University of Helsinki, J.A. Palménintie 260, 10900 Hanko, Finland

HIGHLIGHTS

- Estuarine trace metal processing was studied using sediment geochemical methods.
- Terrestrial organic matter input drives estuarine trace metal accumulation.
- Accumulation of terrestrial organic matter and trace metals peaked in the 1970s.
- Diagenetic processes transform trace metals into more refractory phases.
- Refractory metal-OM complexes comprise a permanent trace metal sink in the estuary.

GRAPHICAL ABSTRACT

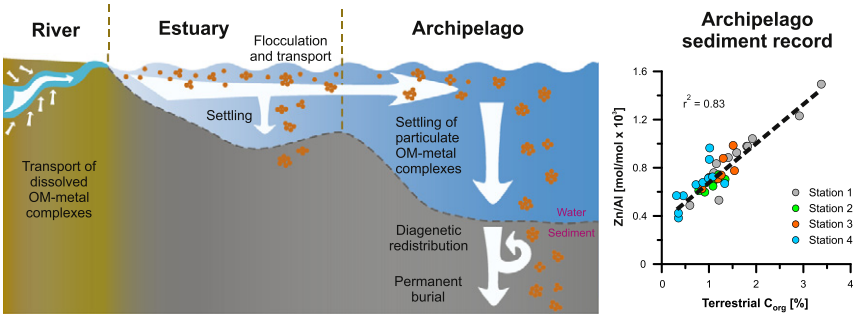

ARTICLE INFO

Article history:
Received 16 December 2019
Received in revised form 29 January 2020
Accepted 30 January 2020
Available online 1 February 2020

Editor: Filip M.G. Tack

Keywords:
Trace metals
Terrestrial organic matter
Diagenesis
Estuary
Sequential extraction
Baltic Sea

ABSTRACT

Coastal sediments play a fundamental role in processing anthropogenic trace metal inputs. Previous studies have shown that terrestrial organic matter (OM) is a significant vector for trace metal transport across the land-to-sea continuum, but little is known about the fate of land-derived metal-OM complexes in coastal sediments. Here, we use a comprehensive set of sediment pore water and solid-phase analyses to investigate how variations in terrestrial OM delivery since the 1950s have influenced trace metal accumulation and diagenesis in a human-impacted boreal estuary in the northern Baltic Sea. A key feature of our dataset is a strong correlation between terrestrial OM deposition and accumulation of metal-OM complexes in the sediments. Based on this strong coupling, we infer that the riverine input of terrestrial metal-OM complexes from the hinterland, followed by flocculation-induced settling in the estuary, effectively modulates sedimentary trace metal sequestration. While part of the trace metal pool associated with these complexes is efficiently recycled in the surface sediments during diagenesis, a substantial fraction is permanently buried as refractory metal-OM complexes or through incorporation into insoluble sulfides, thereby escaping further biological processing. These findings suggest that terrestrial OM input could play a more pivotal role in trace metal processing in coastal environments than hitherto acknowledged.

* Corresponding author at: Aquatic Biogeochemistry Research Unit, Ecosystems and Environment Research Program, Faculty of Biological and Environmental Sciences, University of Helsinki, P.O. Box 65, FI-00014 Helsinki, Finland.
E-mail address: sami.jokinen@utu.fi (S.A. Jokinen).

https://doi.org/10.1016/j.scitotenv.2020.137047

1. Introduction

Excess human-induced trace metal(loid) (henceforth simply referred to as trace metals) loading to aquatic environments may entail serious risks to coastal ecosystems and human health due to their toxicity, persistence and effective bioaccumulation in food chains (Rainbow, 2007; Rainbow and Luoma, 2011; Yi et al., 2011; Amato et al., 2015; Richir and Gobert, 2016). Due to the intensive urbanization along coastlines, human-induced trace metal input is particularly high in estuarine and coastal aquatic environments (Nobi et al., 2010; Pan and Wang, 2012; Gao et al., 2014; Emili et al., 2016; Schintu et al., 2016). Anthropogenic trace metal loading results from various industrial, agricultural, and urban activities (e.g. mining and smelting, fossil fuel combustion, use of fertilizers and pesticides, and municipal waste incineration), which deliver contaminants to the environment either through atmospheric or aquatic input, thereby adding to the trace metal pool naturally present in soils and sediments (Nriagu, 1979; Callender, 2005; Roos and Åström, 2005; Pacyna et al., 2005; Wei and Yang, 2010). Along with the rapid economic development after the Second World War, massive quantities of trace metals have been released to the environment particularly since the 1950s (Callender, 2005). Therefore, constraining the processes that dictate the fate of trace metals in the environment is fundamental in search of effective measures to mitigate degradation of both aquatic and terrestrial ecosystems.

While part of the land-based anthropogenic trace metal pool is effectively retained in the catchment soils and sediments, a substantial fraction is eventually carried to the coastal zone via river runoff (Callender, 2005). In rivers and streams, trace metals are carried in dissolved, colloidal or particulate form primarily in association with organic matter, Fe—Mn (oxyhydr)oxides and clay particles, which are ubiquitous in the aquatic environment and possess a high metal sorption capacity (Singh and Subramanian, 1984; Parker and Rae, 1998; Warren and Haack, 2001; Pokrovsky and Schott, 2002; Hassellöv and von der Kammer, 2008; Nystrand et al., 2012). In the coastal zone, these river-borne constituents become exposed to multitudinous sorption/desorption, flocculation/deflocculation and aggregation/breakup processes, which often lead to non-conservative behavior of trace metals across estuarine gradients (Sholkovitz, 1978; Boyle et al., 1977; Millward, 1995; Dassenakis et al., 1997; Premier et al., 2019). In these processes, the fate and environmental effects of associated trace metals are largely dependent upon their speciation, which directly influences metal reactivity, bioavailability, and toxicity (Passos et al., 2010; Canuto et al., 2013). Indeed, it is widely acknowledged that the ecological consequences of trace metals are primarily governed by metal speciation rather than total concentration (Allen et al., 1980; Liu et al., 2008; Rainbow and Luoma, 2011; Sundaray et al., 2011; Pejman et al., 2017). The most harmful forms of trace metals are free ionic species which are extremely mobile and readily bioavailable (Sunda and Lewis, 1978; Luoma, 1983), whereas at the other end of the spectrum, trace metals hosted in the crystal lattice of silicate minerals are generally inert and non-bioavailable (Tüzen, 2003). Overall, trace metal species sourced from anthropogenic activities are more mobile than the lithogenic background pool of metals (Salomons and Förstner, 1980; Yuan et al., 2004; Heltai et al., 2005; Passos et al., 2010) and hence more readily enter aquatic food chains.

Estuarine flocculation and aggregation processes stimulate the flux of particulate biogenic and lithogenic material and associated trace metals to the seabed (Boyle et al., 1977; Sholkovitz, 1978; Davis, 1984; Gibbs, 1986). As a result, sediments comprise a key sink and source of trace metals in coastal aquatic environments, serving as a locus for storage and redistribution of these substances (e.g. Elderfield and Hepworth, 1975). A major driver of trace metal recycling in coastal sediments is microbially driven oxidation of OM and associated reductive dissolution of Fe—Mn (oxyhydr)oxides (organo-clastic reduction) (Shaw et al., 1990; Audry et al., 2006; Tankere-Muller et al., 2007; Santos-Echeandia et al., 2009; Prajith et al., 2016). In OM-rich coastal sediments a network of primary and secondary diagenetic reactions linked to mineralization of OM (Kraal et al., 2012) occurs within a few centimeters from the sediment-water interface, inducing steep gradients in pore water O_2, pH and H_2S_{aq} levels (Canfield et al., 1993; Sawicka and Brüchert, 2017; Silburn et al., 2017). Alongside the diagenetic remobilization of trace metals directly associated with OM and/or Fe—Mn (oxyhydr)oxides, these gradients may also induce dissolution of other reactive metal carrying phases (Tankere-Muller et al., 2007), while trace metals hosted by more refractory phases e.g. within crystal lattice of silicate minerals pose little potential for post-depositional mobilization (Tüzen, 2003). While these post-depositional processes efficiently increase pore water trace metal concentrations near the sediment-water interface (SWI) and enhance their efflux to the overlying water column (Emerson et al., 1984; Santos-Echeandia et al., 2009; Emili et al., 2016), secondary diagenetic reactions may also lead to scavenging of dissolved trace metals by precipitation of Fe—Mn (oxyhydr)oxides (Rigaud et al., 2013) or metal sulfides (Huerta-Diaz and Morse, 1992) upon upward or downward diffusion, respectively. On the other hand, mineralization of OM summarily releases dissolved organic matter (DOM) into pore waters, which could stabilize trace metals into the dissolved phase through complexation (Santos-Echeandia et al., 2009; Charriau et al., 2011; Rigaud et al., 2013; Dang et al., 2015; Olson et al., 2017). Taken together, these diverse post-depositional processes demonstrate that robust assessment of ecological risks posed by the sedimentary pool of trace metals clearly requires solid understanding of their syn-depositional speciation and diagenetic processing.

In the context of ecological risk assessment and processing of trace metals in estuaries, an important emerging paradigm is that dissolved (or colloidal) organic matter plays a key role in trace metal transport across the land-sea continuum in boreal catchments (Wällstedt et al., 2010; Huser et al., 2011; Lidman et al., 2014). This is principally ascribed to the strong metal complexing capacity of humic and fulvic substances that generally constitute a major fraction of the terrestrial DOM pool (Benedetti et al., 1996; Leenheer et al., 1998; Yang and van der Berg, 2009). Furthermore, it has been demonstrated that flocculation of DOM in the estuarine environments may stimulate sedimentation of metal-OM complexes derived from the terrestrial environment (Sholkovitz, 1978; Sholkovitz et al., 1978; Wells et al., 2000; Turner et al., 2002; Stolpe and Hassellöv, 2007; Biati et al., 2010; Samani et al., 2014; Heidari, 2019). However, despite the putatively significant role of terrestrial OM in trace metal transport and burial in the coastal zone, few studies have hitherto addressed the ultimate fate of riverine metal-OM complexes in estuarine sediments (Chakrabotry et al., 2016). This oversight is notable since the mode of metal-OM complex input from the terrestrial environment could effectively modulate trace metal processing in the coastal zone. Furthermore, this key gap in knowledge is underpinned by the current trajectory of increasing DOM concentrations in inland surface waters in the northern hemisphere (Ekström et al., 2011; Evans et al., 2012; Oni et al., 2013; Lepistö et al., 2014), which could affect trace metal delivery to coastal areas in the future.

In this study, we investigate how decadal-scale temporal variations in terrestrial OM input since the 1950s have affected trace metal accumulation and diagenetic processing in sediments of a human-impacted boreal estuary in the northern Baltic Sea, where previous studies show evidence for active flocculation (Asmala et al., 2014, 2016) and sedimentation of terrestrial OM (Jilbert et al., 2018) along the estuarine salinity gradient. To this end, we apply a diverse set of solid-phase and pore water analyses to four sediment cores to distinguish temporal changes in trace metal input from the effects of diagenetic overprinting. Specifically, we elucidate downcore changes in trace metal speciation using a five-step sequential extraction procedure (modified from Tessier et al., 1979), and relate these to temporal variations in terrestrial OM input inferred from a nitrogen nitrogen/carbon (N/C)–based binary mixing model. Moreover, we delineate potential sources for trace metal enrichments over the studied time interval.

2. Materials and methods

2.1. Study area and sediment coring

The Finnish coastline along the Gulf of Finland is characterized by a mosaic of islands, capes and bays, intersected by deeper channel-like estuaries mainly trending from north to south (Fig. 1). This heterogeneous topography is a result of multiple glaciations that eroded the Precambrian peneplain (Winterhalter et al., 1981) with spatially contrasting efficiency depending on the rock type and occurrence of old fracture zones in the bedrock (Edelman, 1949). Following its last deglaciation by 12,500 cal. a BP, the area was successively filled by late- and postglacial lacustrine clays, and brackish-water muds, which smooth the underlying topography (Virtasalo et al., 2014a).

The main focus of this study is the Storfjärden basin in the Finnish coastal zone (Fig. 1B). The basin is part of the archipelago region of the non-tidal Pojo Bay estuarine system, the recipient of the river Mustionjoki (annual mean discharge 15 $m^3\ s^{-1}$, total suspended solids 5.5 mg L^{-1}, data from Finnish Environment Institute) that collects waters from a catchment dominated by agriculture and forestry (Fig. 1A). The archipelago is separated from the inner estuary by the shallow sill of the First Salpausselkä ice-marginal formation. Although continuous estuarine circulation is observed in the inner estuary of Pojo Bay (Stipa, 1999), the waters in the archipelago area are only seasonally stratified due to summer irradiation. Storfjärden represents a typical middle archipelago accumulation basin with large parts of the seafloor being covered by recently deposited brackish-water mud (Virtasalo et al., 2019). Accumulation of these muds mainly results from reworking and focusing of the previously deposited clays and muds (Virtasalo et al., 2014a). This sediment input is augmented by the delivery of local phytoplankton-derived OM, which dominates the sedimentary OM pool in the area (Jilbert et al., 2018).

Sediments were collected from four stations in the Storfjärden basin during two sampling campaigns (October 2016 and August 2017) onboard R/V *Saduria* using a GEMAX™ twin-barrel short gravity corer (internal diameter 9 cm, core length 20–60 cm; Table 1; Fig. 1B). At each station in October 2016, one of the duplicate cores was sampled for pore water analyses and the other one was sliced for solid-phase analyses. In August 2017, Stations 1, 2, and 4 were re-sampled for pore water analysis to monitor temporal variations in the diagenetic zonation.

2.2. Pore water analyses

2.2.1. Sampling

Two parallel pore water sample series (henceforth referred to as 'bulk' and 'sulfide' series) were collected from each core through predrilled holes (diameter 4 mm, vertical resolution 2 cm) in the GEMAX™ core tubes using Rhizons™ mounted on a purpose-built plastic rack. The Rhizons™ were directly connected to polyethylene syringes, which were held open with wooden spacers to create a vacuum. During the pore water sampling, we also collected two parallel bottom water samples from the core tubes using the same procedure. The sulfide series syringes were pre-filled with 1 mL of 10% zinc acetate solution to trap the pore water sulfide as ZnS. Within 2 h of retrieval, all samples were transferred from the syringes to 15 mL centrifuge tubes. Subsequently, an aliquot was immediately taken from the bulk series samples and acidified to 1 M HNO_3 for elemental analysis by ICP-OES, while the rest was used for ammonium (NH_4^+) measurements.

2.2.2. Concentration measurements

Total sulfide (ΣS^{2-}) concentration in the pore water was measured spectrophotometrically (670 nm) from the sulfide series samples after direct addition of an acidic solution of $FeCl_3$ and *N*, *N*-dimethyl-*p*-phenylenediamine (Cline, 1969; Reese et al., 2011) to sample vials. The method is founded on dissolution of the ZnS precipitate upon acidification and subsequent quantitative complexation of S as methylene blue (Jilbert et al., 2018). A series of standard solutions of $Na_2S{\cdot}3H_2O$ fixed in Zn acetate similarly to the samples were used to calibrate the measurements through quantification of the exact S concentration in the stock solution by iodometric titration (Burton et al., 2008). The non-acidified bulk series samples were analyzed for pore water NH_4^+ concentration by spectrophotometry following methods described in Koistinen et al. (2018). Elemental concentrations in the pore water were determined from the acidified bulk series samples by ICP-MS (Thermo Fisher Scientific) at Utrecht University Department of Earth Sciences. Due to the sample acidification, Iron (Fe), manganese (Mn), phosphorus (P), and sulfur (S) are assumed to be present as Fe^{2+}, Mn^{2+}, HPO_4^{2-}, and SO_4^{2-}, respectively (Jilbert and Slomp, 2013). For all of the techniques, replicate measurements of samples and standards indicated analytical precision of <5%.

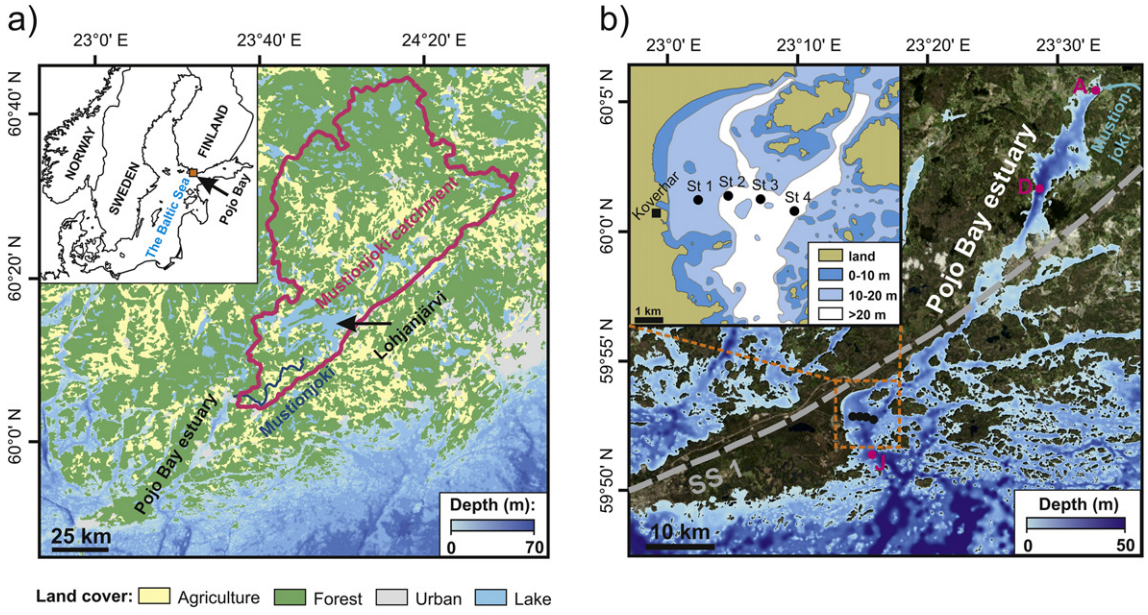

Fig. 1. (A) Distribution of different land cover types in the catchment area (purple line) of Pojo Bay. (B) Bathymetric map of the Pojo Bay estuarine system and adjacent coastal area with a more detailed map of the Storfjärden area in the inset. The principal data of this study was obtained from Storfjärden coring sites (black circles). Additional study sites from Jilbert et al. (2018) (see Fig. S4) are also shown (purple circles).

Table 1
Sampling locations and conducted analyses.

Station	Latitude (WGS 84)	Longitude (WGS 84)	Water depth (m)	Pore water analyses	Solid-phase analyses
St 1	59.880000	23.235917	16.5	October 2016 August 2017	October 2016
St 2	59.880667	23.245500	22.0	October 2016 August 2017	October 2016
St 3	59.880133	23.255750	22.0	October 2016	October 2016
St 4	59.878200	23.266517	23.0	October 2016 August 2017	October 2016

2.3. Solid-phase analyses

The sediment cores retrieved for solid-phases analyses were sliced at 1 cm resolution for the topmost decimeter and at 2 cm resolution for the remaining length. The collected sediment slices were immediately transferred into plastic bags and carefully sealed under water. Before further processing, the bags were placed into a gas-tight, N_2-filled glass jar within 1 h of the sectioning and stored in the dark at 4 °C. No visible signs of oxidation during sectioning and storage were observed. The stored sediment slices were later frozen, freeze-dried, and homogenized under N_2. Water content (weight %) was estimated from parallel wet samples by weight loss on freeze-drying.

2.3.1. Carbon and nitrogen content and organic matter source apportionment

Solid-phase contents of carbon (C) and nitrogen (N) in the sediments were analyzed by thermal combustion elemental analysis (TCEA) at Tvärminne Zoological Station (precision and accuracy <2.5%). For the analysis, 3–4 mg of dried and ground sediment was weighted into tin cups and placed into an autosampler rosette. The pools of inorganic C and N are negligible in this setting (Virtasalo et al., 2005; Jilbert et al., 2018), hence no decalcification was conducted and the total contents were considered equal to organic C (C_{org}) and N (N_{org}). To quantify the proportions of terrestrial plant-derived (%OC_{terr}) and phytoplankton-derived OM (%OC_{phyt}) in the C_{org} pool, a simple binary mixing model was applied for the molar N/C ratio assuming end-member values of $(N/C)_{terr} = 0.04$ and $(N/C)_{phyt} = 0.13$ following Goñi et al. (2003) and Jilbert et al. (2018).

$$\%OC_{terr} = \frac{(N/C)_{sample} - (N/C)_{phyt}}{(N/C)_{terr}} - (N/C)_{phyt} \times 100 \quad (1)$$

The model integrates a variety of terrestrial OM sources ranging from fresh vascular plant detritus to more degraded soil OM into a single end-member. This is practical since effectively all of the OM transported by rivers passes through the soil reservoir before entering the coastal zone, hence representing a mixture of variably degraded material (Jokinen et al., 2018). Furthermore, the model assumes that the N/C ratios of the end-members are temporally and spatially fixed and that these values remain virtually unaltered during sedimentation and burial of OM.

2.3.2. Total elemental contents

For the quantification of total elemental contents (S and metals) in the solid-phase, dried and homogenized samples were subjected to a triple-acid digestion procedure. 0.1–0.2 g of sediment was dissolved in 2.5 mL of HF (38%) and 2.5 mL of a mixture of $HClO_4$ (70%) and HNO_3 (65%) (volumetric ratio 3:2) in closed Teflon bombs at 90 °C for 12 h. After evaporation of the acids at 160 °C, the resulting gel was dissolved in Suprapur^R 1 M HNO_3 and analyzed for metal contents by ICP-MS. Precision and accuracy of the analysis were <5% based on calibration to standard solutions and checking against a quality control standard. Reproducibility of the total extraction procedure determined by replicates was <5% for all elements except Fe and Sn (<15%). Absolute accuracy of the entire sample preparation, digestion, and analysis, as determined by comparison with standard reference material ISE-921 (Van der Veer, 2006), was <15% for all elements except Pb, Cd, and As (<25%).

2.3.3. Sequential extraction of metals

To investigate the solid-phase partitioning of metals, an aliquot of 0.2–0.3 g of dried and homogenized sediment was subjected to a four-step sequential extraction procedure combining aspects of the protocols of Tessier et al. (1979), Poulton and Canfield (2005), and Ruttenberg (1992) (Table 2). During the first two stages (fractions F1 and F2) of the extraction protocol, the samples were kept in a glove bag under N_2 to avoid oxidation artefacts. The extractions were conducted in centrifuge tubes placed into an orbital shaker (300 rpm) to agitate the reaction. Following each extraction step, the samples were centrifuged (2500 rpm, 5 min) and the supernatant collected for analysis either by ICP-MS (F1, F2, F4) or ICP-OES (F3). After the stage F3, the samples were transferred to crucibles with UHQ water, taken to dryness on a hot plate and incinerated at 550 °C for 2 h. The incinerated samples were transferred back to centrifuge tubes using 1 M HCl, after which the extraction procedure continued as in stages F1–F3. The residual fraction F5 was quantified by subtracting the sum of the fractions F1–F4 from the total content. Finally, due to a suspected contamination, all solid-phase Cu data from Station 3 was discarded. For both ICP-OES and ICP-MS measurements, analytical precision was <5%. Reproducibility of the sequential extraction procedure determined by replicates was generally better than 10%.

Following the approach of Jilbert et al. (2018), in this study we use the terms labile/refractory to describe the chemical reactivity of metal host phases as determined by sequential extraction, noting that in reality a continuum of reactivity of such phases exists in the sediments. Specifically, we refer to phases extracted in fractions F1, F2, and F3 as labile, whereas the fractions F4 and F5 are classified as refractory. We note that this division differs slightly from Jilbert et al. (2018) in that the dithionite-soluble phases (F3) are here classed as labile, whereas in Jilbert et al. (2018) these were classed as refractory. This classification is justified by the similar diagenetic behavior of phases extractable in F1–F3 in the present study (Section 4.4).

2.3.4. ^{137}Cs analysis and core correlation

To locate the Chernobyl-derived peak in ^{137}Cs activity denoting the year 1986 in the sediment profiles, gamma spectra of the remaining wet sediment samples from Stations 1 and 4 were measured at the Geological Survey of Finland using an BrightSpec bMCA-USB pulse height analyzer equipped with a well-type NAI(Tl) detector. Due to the potential post-depositional downward transport of ^{137}Cs through bioturbation and diffusion (Holby and Evans, 1996; Klaminder et al., 2012) the depth of peak ^{137}Cs activity (rather than the initial increase) was assumed to represent the Chernobyl-derived fallout (e.g. Ojala et al., 2017). As the aim was only to identify a relative maximum in ^{137}Cs activity, no further corrections were applied to the obtained profiles (Jokinen et al., 2015). Finally, assuming a constant linear sedimentation rate, the obtained ^{137}Cs-based age constraints for Stations 1 and 4 were transferred to Stations 2 and 3 via correlation of the C/N profiles (Fig. S1).

Table 2
Sequential extraction procedure and summary of the relevant phases in each fraction. Note that due to the wide spectrum of metal-binding ligands associated with terrestrial and phytoplankton-derived organic matter (OM), the metal-OM complexes span over fractions F2–F4. Based on their chemical reactivity and diagenetic behavior, these complexes are classified either as labile (F2 and F3) or refractory (F4).

Fraction	Operational description	Reagents	Major phases	References
F1	Exchangeable	$MgCl_2$ (1 M)	Weakly-sorbed metal species	Tessier et al., 1979
F2	Acid-soluble	Na-acetate (1 M), Acetic acid, pH 4.5	Carbonates AVS Labile Me-OM complexes	Tessier et al., 1979 Cornwell and Morse, 1987 Jilbert et al., 2018
F3	Reducible	Na-dithionite (5 wt%), Acetic acid (0.35 M), Na-citrate (0.2 M), pH 4.8	Fe and Mn (oxyhydr)oxides Labile Me-OM complexes	Poulton and Canfield, 2005 Lalonde et al., 2012
F4	Organic	Heating to 550 °C, HCl (1 M)	Refractory Me-OM complexes	Ruttenberg, 1992
F5	Residual	–	Silicates Pyrite	Poulton and Canfield, 2005 Inferred
–	Total	HF (40%) $HClO_4$:HNO_3 (3:2 vol%)		

2.4. Principal component analysis

In order to investigate the main structures in the produced multivariate data, a principal component analysis (PCA) was conducted for the pore water and solid-phase data using R software (R Core Team, 2017). To overcome closed sum effects typical for compositional data, a centered log-ratio transformation was applied to all variables prior to the PCA (Reimann et al., 2008). As a substantial fraction of pore water Cd, Pb, and Sn concentration were below the detection limit, these variables were excluded from the pore water PCA. Similarly, Cu was excluded from the solid-phase PCAs due to the lack of data from Station 3 (Section 2.3.3).

3. Results

3.1. Pore water profiles

3.1.1. General diagenetic zonation

At all stations, the profiles of major pore water constituents (SO_4^{2-}, ΣS^{2-}, NH_4^+, HPO_4^{2-}, Fe^{2+} and Mn^{2+}) display a broadly similar pattern (Fig. 2) that conforms to the classical diagenetic zonation of coastal sediments, reflecting sequential consumption of electron acceptors linked to microbial OM oxidation (e.g. Froelich et al., 1979). A comprehensive description of this zonation in the sediments of the Pojo Bay system was recently provided by Jilbert et al. (2018), hence the main characteristics are only briefly outlined below.

Since oxygen penetration in these OM-rich coastal sediments is generally restricted to the topmost 5 mm (Hietanen and Kuparinen, 2008; Bonaglia et al., 2013), the pore water chemistry is principally dictated by anaerobic diagenetic process. Irrespective of the sampling occasion, ongoing diagenetic mineralization of OM is expressed in the pore water profiles as progressive gradual downward increases in NH_4^+ and HPO_4^{2-} concentrations (Fig. 2). Meanwhile, systematic near-surface peaks in Fe^{2+} paralleled by a subtle build-up of Mn^{2+} at the depth of 0–10 cm denotes organo-clastic reduction of Fe and Mn (oxyhydr)oxides, respectively.

Below the front of organo-clastic reduction of Fe and Mn (oxyhydr) oxides (henceforth referred to as the zone of OCR-Fe-Mn), accumulation of dissolved sulfide is observed in the pore water coincident with an abrupt drawdown of Fe^{2+} and a concave decrease in SO_4^{2-} (Fig. 2). These features indicate SO_4^{2-} reduction and transition into the sulfate-methane transition zone (SMTZ) at the depth of 5–10 cm. Within this front, dissolved Fe pool is exhausted by sulfide due to intense SO_4^{2-} reduction in association with oxidation of OM and upward-diffusing methane (CH_4, not measured in this study). Based on the depletion of Fe^{2+} and accumulation of sulfide, the upper boundary of the SMTZ remains broadly fixed between the two sampling campaigns, except for Station 1. In general, the length of the pore water profiles is insufficient to determine the lower boundary of the SMTZ, with the exception of the Station 2 in 2017, where it lies at the depth of 12 cm, as evidenced by the depletion of ΣS^{2-}.

3.1.2. Trace metal profiles

Despite considerable element-specific variation in depth distribution of pore water trace metals depending on station and sampling campaign, we can broadly distinguish two different groups of profiles (Figs. 3 and 4A). The majority of the studied trace metal profiles in the dissolved phase (As, Cd, Co, Cu, Ni, Pb, Sn, and Zn) generally display highest concentrations above the SMTZ, being characterized either by a peak at the sediment-water interface followed by an exponential decrease with depth (e.g. As, Cr, Ni, Sn at Station 1 in 2016) or by a pronounced subsurface maximum broadly within the zone of OCR-Fe-Mn (e.g. As, Co, at Station 3 in 2016) (Fig. 3). At the transition to the SMTZ, the concentrations of these trace metals generally decrease to consistently lower levels, although occasional deep enrichments are observed within this zone (e.g. As and Cu, at Station 1 in 2016). This general pattern of relatively high concentrations in the zone of OCR-Fe-Mn, followed by a rapid drawdown at the transition to SMTZ causes these profiles to resemble those of SO_4^{2-} (Fig. 4A).

By contrast to the other trace metals, the pore water profiles of Cr and V are generally typified by low concentrations above the SMTZ. The concentrations of these metals increase progressively with depth, whereby the steepest gradient occurs at the transition to the SMTZ. This behavior causes these profiles to more closely resemble those of NH_4^+, HPO_4^{2-}, ΣS^{2-} and Mn (Figs. 2, 3, and 4A).

3.2. Solid-phase profiles

3.2.1. C_{org} and total S profiles

Solid-phase C_{org} content in the sediment is generally in the range 4–5%. (Fig. 5A). Based on the N/C-based mixing model, phytoplankton-derived OM constitutes on average ~70–85% of the C_{org} pool at each station, with an increasing share due to distance from the shore. In the depth profiles, the content of phytoplankton-derived C_{org} generally increases towards the core top at all stations, whereas terrestrial C_{org} exhibits a more complex pattern. Typically, terrestrial C_{org} content is low at the lowermost part of the cores, followed by a pronounced interval of enhanced terrestrial OM accumulation at the core depth of 5–25 cm (around year 1970) and subsequent decrease towards the sediment surface.

Solid-phase total S content generally ranges from 0.5 to 1.5% (Fig. 5B). Downcore variations in total S are characterized by relatively high values in the lower part of the cores (within the SMTZ), followed by a marked upward decrease between 0 and 10 cm core depth (within the zone of OCR-Fe-Mn). The molar ratio of Fe/S in the sediment is in the

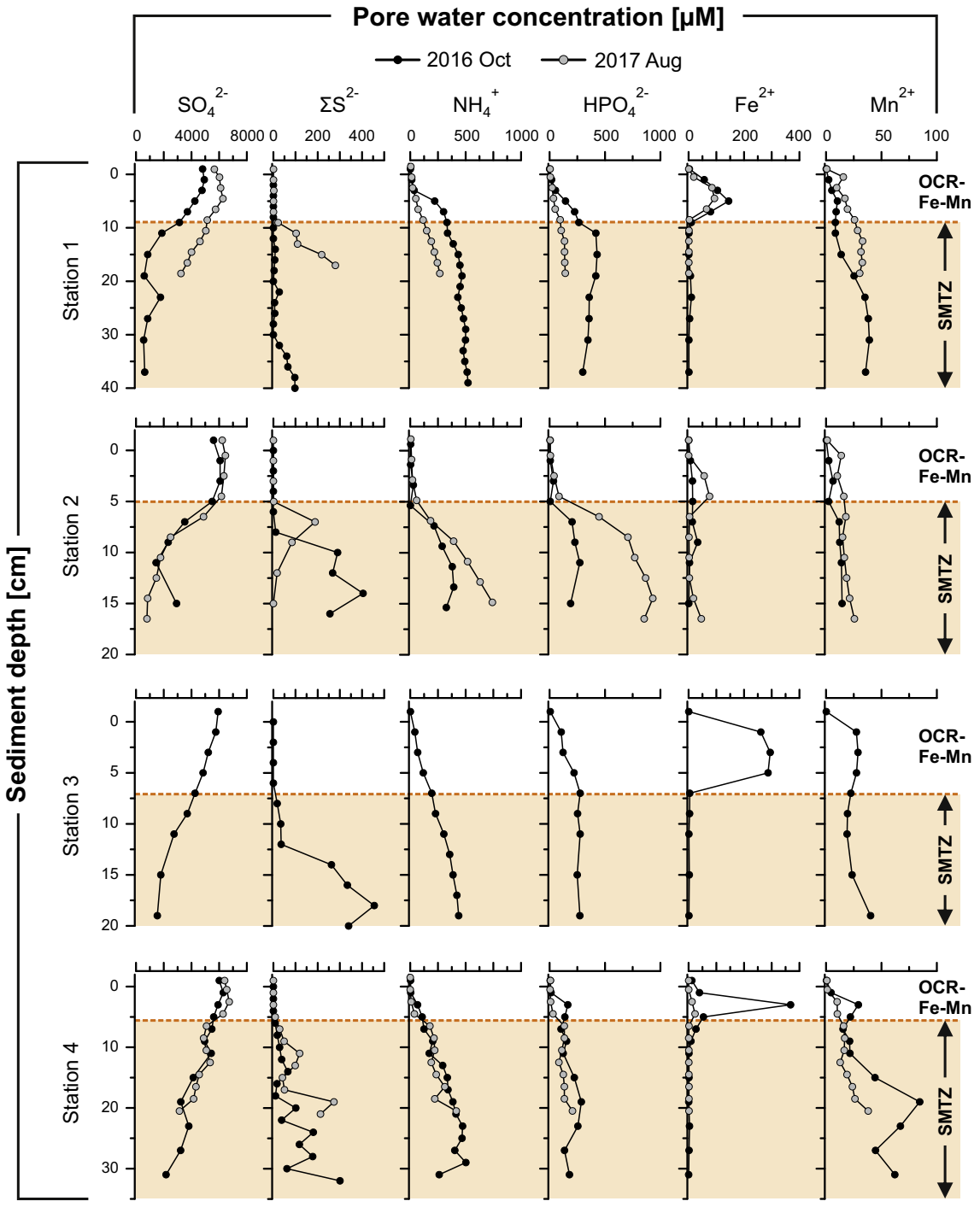

Fig. 2. Downcore profiles for major constituents in the pore waters. OCR-Fe-Mn and SMTZ denote the zones of organo-clastic reduction of Fe—Mn (oxyhydr)oxides and sulfate-methane transition, respectively. Light brown shading illustrates the widest extent of the SMTZ (defined based on the ΣS^{2-} and Fe^{2+} profiles) between the two sampling occasions.

range 2–6. In general, Fe/S is inversely related to total S content, displaying constantly low values within the SMTZ, followed by a substantial increase in the topmost decimeter of the cores.

3.2.2. Average speciation of metals

Based on averages over the sequential extraction data set (combining the profiles from all stations), a major proportion of the total elemental content for all the studied elements resides in the most refractory fractions F4 and F5 (Fig. 6). Specifically, F4 is the dominant fraction for As, Co, Cu, Ni and Zn, while F5 constitutes most of solid-phase Cd, Cr, Fe, Mn, Pb, Sn, and V.

Because F3 was measured by ICP-OES, the contents of several elements in this fraction were generally below the detection limit (Co, Ni, and V) or not measured at all (As, Cd, Pb, and Sn). By definition, this implies that any As, Cd, Pb or Sn present in F3 appears to reside in F5 of our sequential extraction scheme, potentially resulting in overestimation of the residual pool of these elements. Among the quantified elements in F3, this is a substantial fraction of solid-phase Cu (24%) and Zn (16%), whereas it constitutes a smaller but still appreciable fraction of Cr, Fe and Mn (5–10%), and is generally insignificant for Co, Ni, and V. Indeed, based on the limits of quantification for Co, Ni, V in the ICP-OES measurements, the potential cross over from F3 to F5 is <2–5% of the total

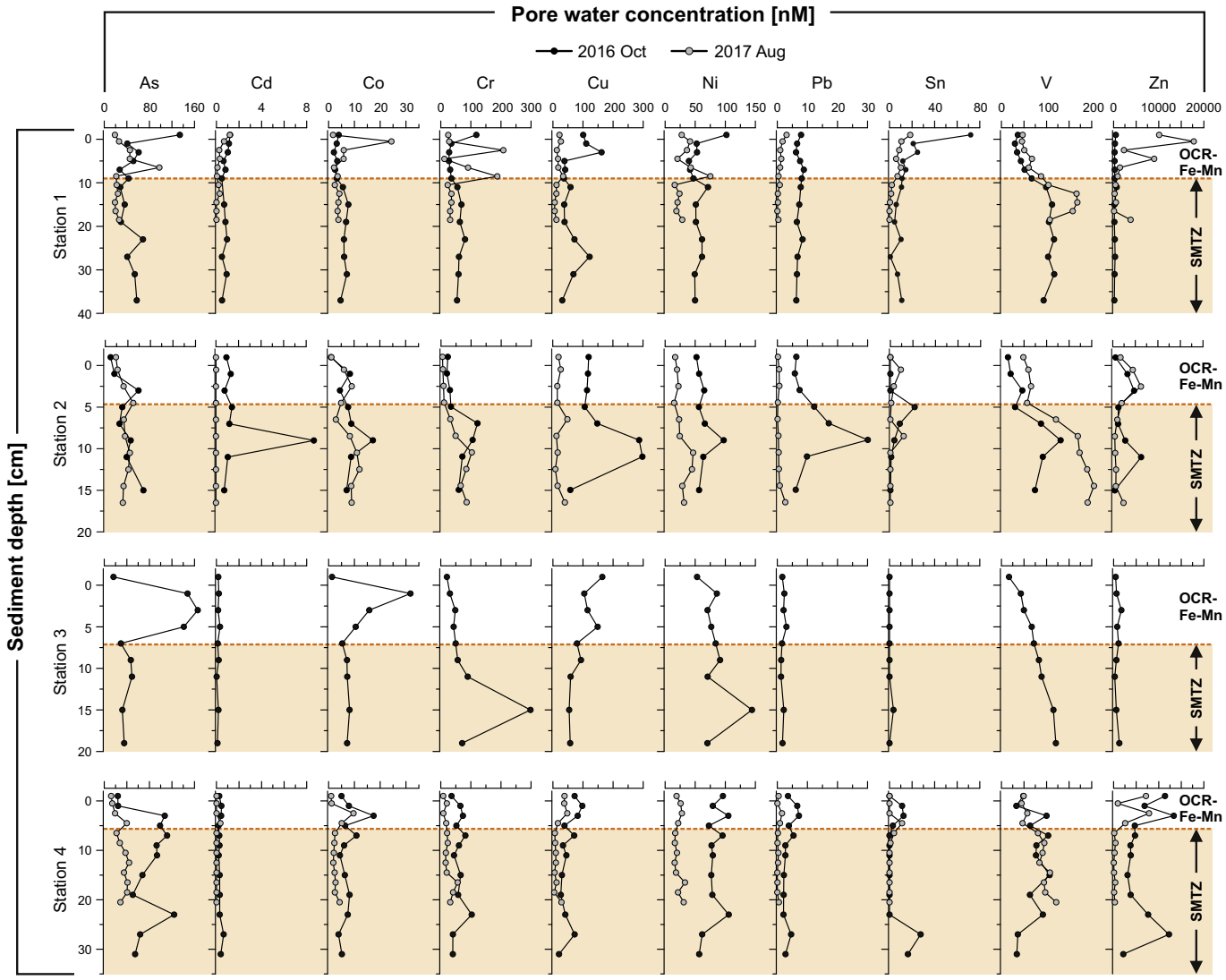

Fig. 3. Pore water trace metal profiles. Diagenetic zonation as in Fig. 2.

content, and therefore not significantly contributing to the content of these trace metals in F5. For As, Cd, Pb and Sn, we cannot quantify the potential propagation from F3 to F5.

F2 constitutes a notable fraction of the solid-phase As, Cd, Pb, and Zn pools (~20–30%), whereas it is a less significant fraction for Co, Fe, Mn, and Ni (~5–10%) and insignificant for Cr, Cu, and Sn (≪5%). By contrast to the other fractions, F1 is generally an insignificant fraction for all metals except for Mn, for which it constitutes 11% of the total solid-phase pool.

3.2.3. Downcore variations in metal speciation

Below we describe the key patterns in depth-variations in solid-phase metal speciation with respect to the general diagenetic zonation (Section 3.1.1) and changes in terrestrial OM input (Section 3.2.1). For the sake of clarity, we group the metals based on the identified key patterns: (1) metals exhibiting a surface enrichment in fractions F1–F3 (Fe, Mn); (2) metals characterized by a downward sink-switch towards more refractory phases (As, Co, Cu, Ni); (3) metals that are strongly coupled with terrestrial C_{org} (Cd, Pb, Sn, Zn); metals with no marked depth-variations in their speciation (Cr and V).

Despite the general decoupling of total solid-phase Fe and Mn, with no marked depth-related trends in Fe, while Mn content generally increases with depth, changes in their speciation within the zone of OCR-Fe-Mn are markedly similar (Fig. 7). Specifically, both metals exhibit a surface enrichment followed by downward decrease in the labile fractions F1–F3. Within the SMTZ, however, downcore variations in Fe and Mn speciation become more decoupled; Fe generally displays a pronounced maximum in F2 and F3 at the depth interval of enhanced terrestrial OM accumulation (cf. Cd, Pb, Sn and Zn), while Mn sequestration in fractions F1–F3 shows a progressive downward increase towards the core bottom. With respect to F5, accumulation of both Fe and Mn gradually increases with depth.

Although no general pattern is observed in the depth profiles for the total content of As, Co, Cu, and Ni, downcore variations in their speciation are broadly similar (Fig. 7). Within the zone of OCR-Fe-Mn, these trace metals behave similarly to Fe and Mn, displaying a near-surface enrichment and subsequent decline with depth in the labile fractions (F2 and F3). Within the SMTZ, As, Co, Cu, and Ni exhibit a gradual downward sink-switch primarily from the labile fractions F2 and F3 to the most refractory fraction F5. Overall, this sink-switch is most prominent at the transition to the SMTZ especially at Stations 2 and 4, where also the surface-enrichment of Co and Cu in fractions F2 and F3 is most pronounced.

A prominent feature of the solid-phase profiles for Cd, Pb, Sn and Zn is their co-variation with terrestrial C_{org} with respect to both total content and speciation, the pattern being most pronounced at Stations 1

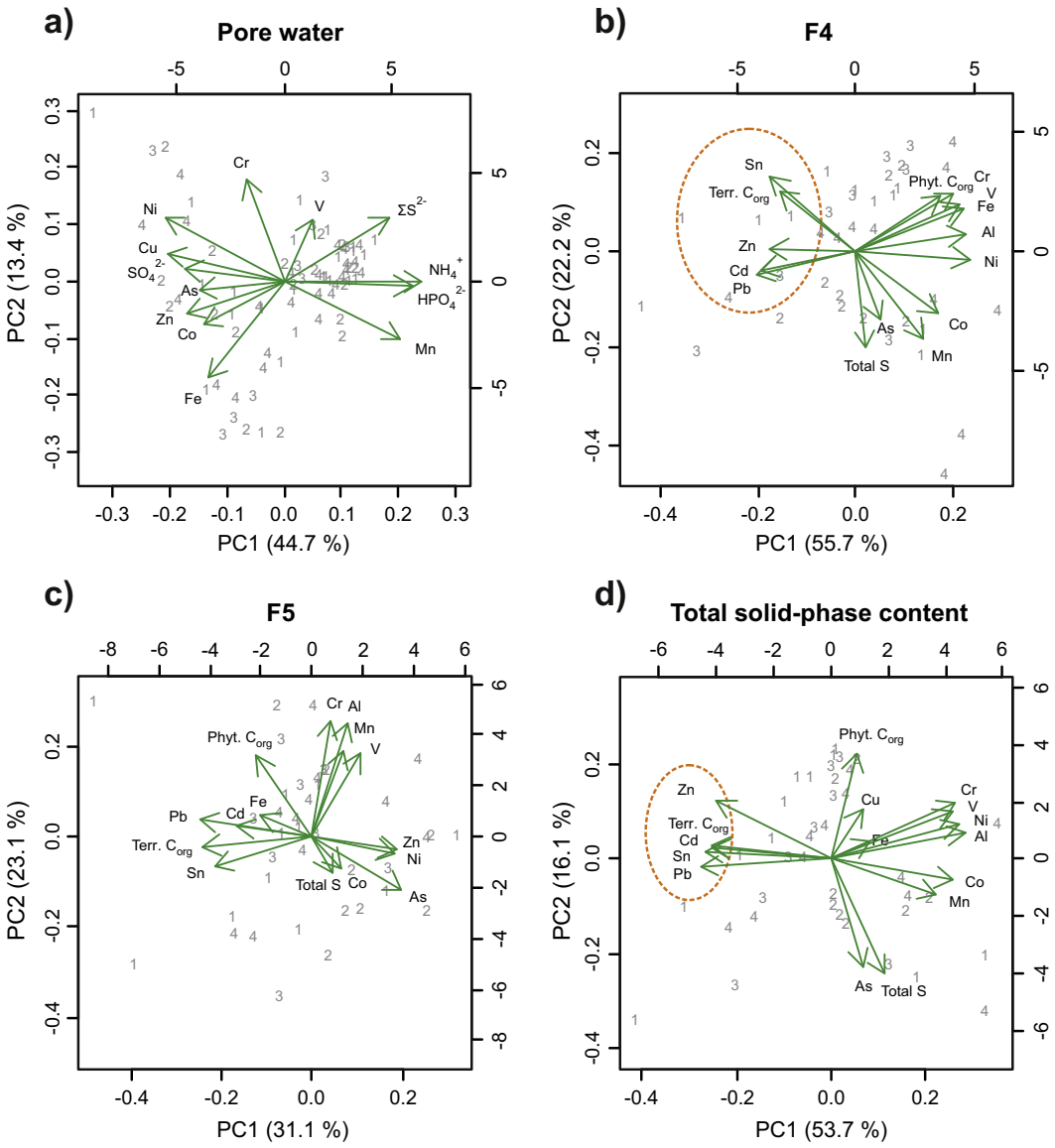

Fig. 4. Biplots of principal component analyses for pore water constituents (A) and solid-phase contents in fractions F4 (B) and F5 (C) as well as for the total solid-phase content (D). Note the clustering of terrestrial C_{org} and Cd, Pb, Sn, and Zn in F4 and in the total solid-phase content (orange ellipses).

and 4 (Figs. 4D, 7, and 8). Specifically, sequestration of these metals peaks within the interval of enhanced terrestrial C_{org} accumulation centered around 1970s due to their increased uptake into fractions F2–F4 (Figs. 7 and 8). Superimposed on this general pattern, Cd (all stations) and Zn (Stations 2 and 4) displays a prominent near-surface enrichment in F2 within the zone of OCR-Fe-Mn, which is decoupled from variations in terrestrial C_{org} content.

Finally, solid-phase Cr and V profiles display negligible depth-variability neither in the total content nor in the speciation.

4. Discussion

4.1. Inferred speciation in the sequential extraction procedure

4.1.1. Fraction 1

The $MgCl_2$ extractable fraction F1 is thought to comprise extremely labile, weakly-sorbed metal species that are readily released from the sediment by ion-exchange processes (e.g. Tessier et al., 1979; Gleyzes et al., 2002), retaining sulfides, OM and silicates virtually intact during extraction (Tessier et al., 1979; Pickering, 1986). Although partial dissolution of carbonates and Mn oxides by $MgCl_2$ due to pH reduction might occur (Bordas and Bourg, 1998), we infer based on the generally higher proportion of Mn in F1 in comparison to F2 and F3 (Figs. 6 and 7) that such dissolution effects are not substantial. Negligible contribution from dissolution of Mn oxides is further supported by the absence of Fe in F1, since a decrease in pH should also trigger at least partial dissolution of Fe oxides (Pickering, 1986). Therefore, it is likely that F1 predominantly comprises metal species adhered to the sediment particles by weak electrostatic interactions, as targeted. In general, our results add to the existing evidence that this extraction step yields low recovery of trace metals in estuarine sediments owing to the high concentration of cations in seawater, which occupy sorption sites (Burton et al., 2005).

4.1.2. Fraction 2

The Na-acetate extraction at low pH was originally targeted to dissolve carbonate-bound metals while simultaneously leaving silicate and sulfide minerals and OM as intact as possible (Tessier et al., 1979). Based on earlier studies in similar estuaries in the northern Baltic Sea, Mn carbonate phases, especially rhodochrosite, are likely present in the studied samples (Yu et al., 2016), whereas Fe carbonate phases

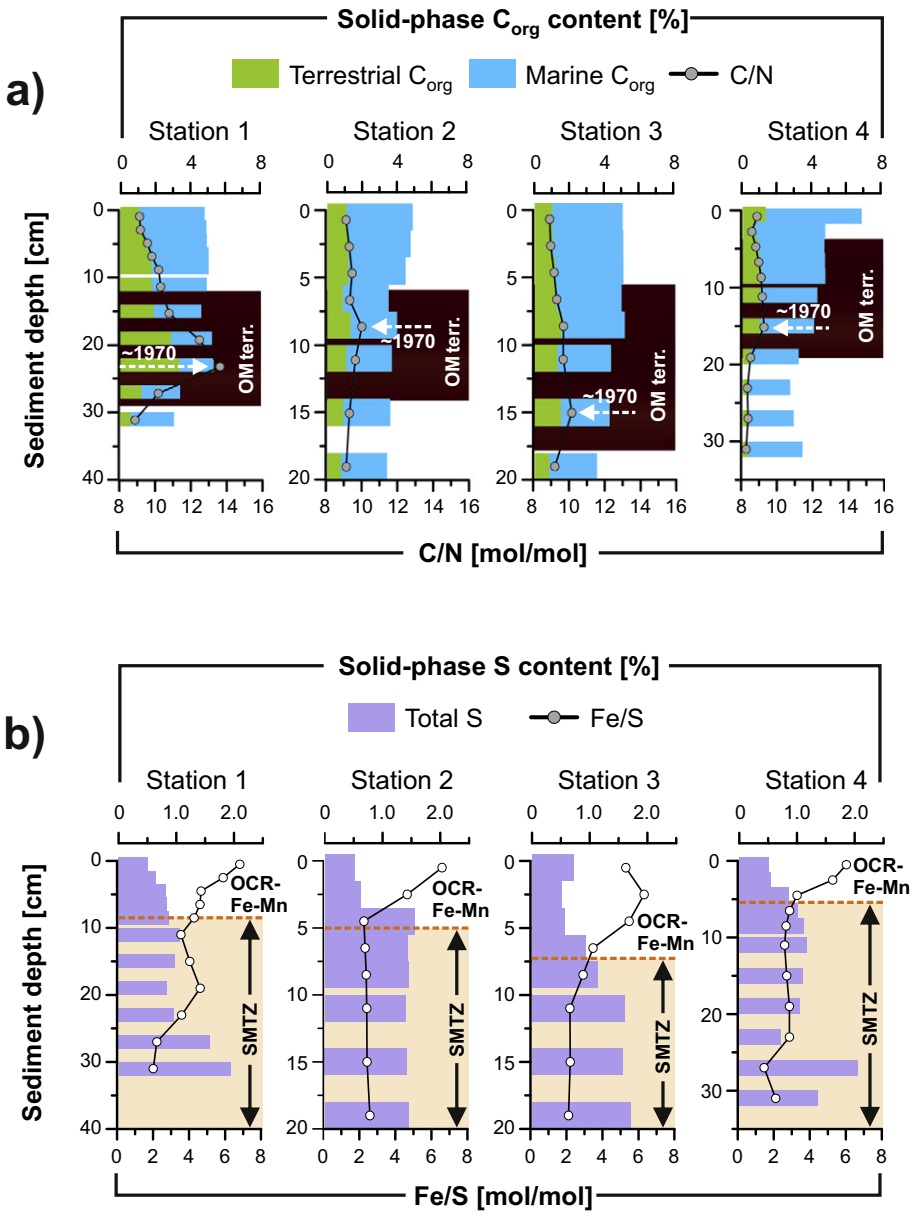

Fig. 5. (A) Downcore variations in terrestrial and phytoplankton-derived C_{org} content calculated from the N/C-based mixing model (see text for details). Violet shading indicates the period of enhanced terrestrial organic matter input around the 1970s. (B) Downcore variations in total solid-phase S content and Fe/S ratio. Diagenetic zonation as in Fig. 2.

such as siderite and ankerite are likely absent (Jilbert et al., 2018). Although Yu et al. (2016), reported only partial dissolution of rhodochrosite in 1 M NH_4-acetate at pH 6, we infer that the markedly lower pH of 4.5 applied here yields a substantially higher recovery. Overall, the generally low content of carbonate minerals in the coastal northern Baltic Sea sediments (Jönsson et al., 2005; Virtasalo et al., 2005; Savage et al., 2010; Jilbert et al., 2018), suggest that carbonates constitute only a minor host phase for trace metals in F2. The absence of authigenic carbonates is related to relatively low concentrations of dissolved inorganic carbon in the surface sediment pore waters, which prevents precipitation of Fe and Mn carbonates above the SMTZ, while the drawdown of Fe^{2+} by high H_2S_{aq} levels sustains undersaturation with respect to Fe carbonates within the SMTZ (Jilbert et al., 2018).

In addition to carbonates, other candidates for trace metal host phases in F2 include acid-volatile sulfides (AVS) (Cornwell and Morse, 1987) and labile metal-OM complexes (Jilbert et al., 2018), both of which are often considered as key sorbents for trace metals in organic-rich estuarine sediments (Lion et al., 1982; Burton et al., 2006a). Indeed, although different AVS phases may dissolve over multiple stages of sequential extraction procedures (e.g. Kheboian and Bauer, 1987; Wallmann et al., 1992; Cooper and Morse, 1998; Burton et al., 2006b), the majority of AVS and associated trace metals can be expected to dissolve at the low pH of this extraction step (Cornwell and Morse, 1987; Poulton and Canfield, 2005). However, building on the work of Yu et al. (2015) on Fe speciation in coastal Baltic Sea sediments, Jilbert et al. (2018) demonstrated that a significant amount of easily extractable Fe in sediments of Pojo Bay is present as unsulfidized Fe (II) complexed with OM. Assuming broadly similar partitioning between Fe and other metals, we therefore interpret the Na-Ace extractable trace metal pool to consist primarily of labile metal-OM complexes.

4.1.3. Fraction 3

The dithionite-citrate couple is commonly used to extract Fe and Mn (oxyhydr)oxides from sediments (Mehra and Jackson, 1958; Anderson

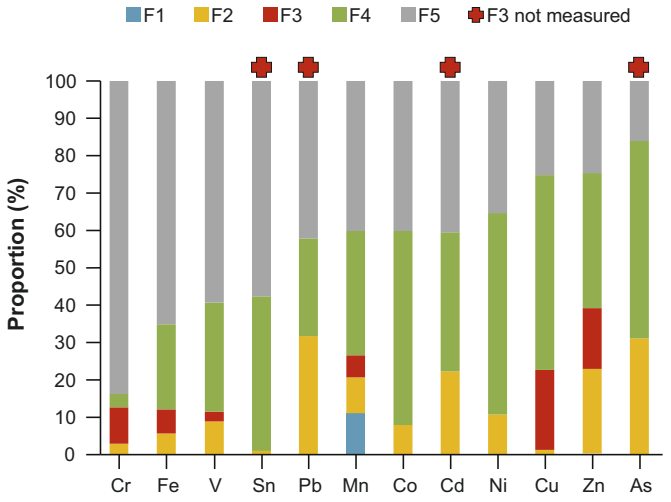

Fig. 6. Average metal speciation in the solid-phase. Description of the operationally defined fractions (F1–F5) in the sequential extraction procedure is given in Table 2. Note that because F3 was measured by ICP-OES, the contents of several elements in this fraction were generally below the detection limit (Co, Ni, and V) or not measured at all (As, Cd, Pb, and Sn).

and Jenne, 1970). In our sequential extraction scheme, Na-dithionite solution was buffered to pH 4.8 with acetic acid and Na-citrate (Mehra and Jackson, 1958), which is a commonly used mixture to extract highly reactive Fe (oxyhydr)oxide phases such as ferrihydrite, lepidocrocite, goethite, and hematite (Poulton and Canfield, 2005). Given that Mn oxides generally dissolve more easily than Fe oxides (Chao, 1972), the quantitative recovery of Fe (oxyhydr)oxides in this extraction step (Raiswell et al., 1994; Poulton and Canfield, 2005) implies effective recovery also for Mn (oxyhydr)oxides. Accordingly, effective dissolution of both Fe and Mn (oxhyhydr)oxides is evidenced by the strong correlation between Fe and Mn in F3 ($r_s = 0.76$, $p < 0.001$) despite their general decoupling in other fractions. This coupling suggests, together with the peaks in Fe and Mn contents in F3 in the near-surface sediments within the zone of OCR-Fe-Mn (Figs. 2 and 7), that Fe and Mn (oxyhydr)oxides are the predominant trace metal host phases in F3. In addition to Fe and Mn (oxyhydr)oxides, labile metal-OM complexes (Lalonde et al., 2012) and AVS that potentially escaped dissolution in the first two extraction steps might also contribute to the trace metal pool in F3 (Jilbert et al., 2018). Of these two candidate host phases, labile metal-OM complexes are likely quantitatively more important for the reasons already outlined for F2 (Section 4.1.2).

4.1.4. Fraction 4

Because strong oxidizing agents conventionally applied to extract OM-bound trace metals tend to at least partially oxidize pyrite (e.g. Gleyzes et al., 2002), we used incineration at 550 °C followed by leaching with 1 M HCl to extract this fraction (Ruttenberg, 1992). We note that the heating likely results in loss of structural water from clay minerals (Ball, 1964), but this is not expected to mobilize trace metals. Likewise, the potential thermal decomposition of siderite and rhodochrosite at this temperature (Weliky et al., 1983) is not relevant here, since these phases are likely to dissolve in the earlier stages of our sequential extraction procedure.

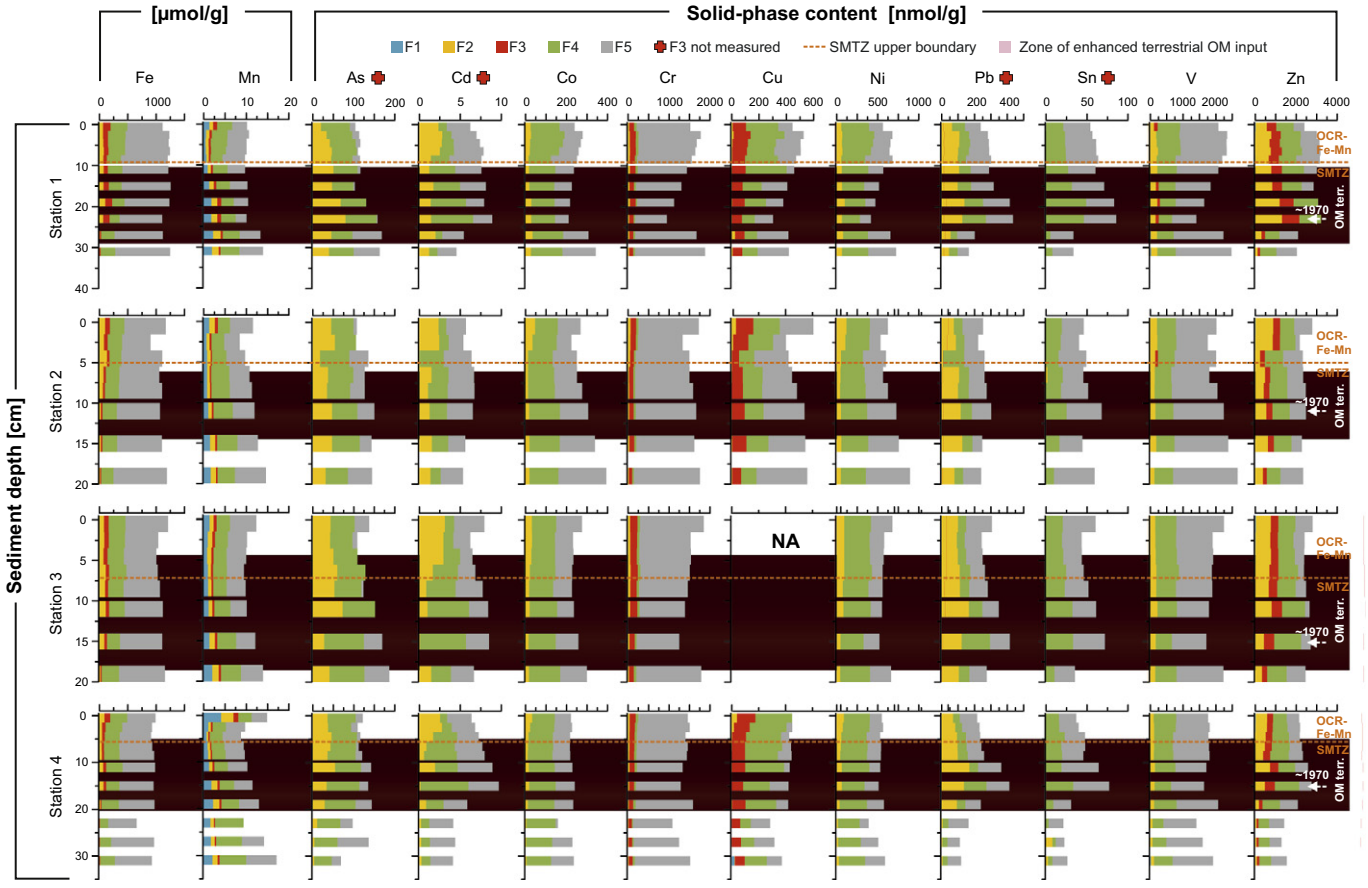

Fig. 7. Downcore variations in metal speciation. Description of the operationally defined fractions (F1–F5) in the sequential extraction procedure is given in Table 2. Note that because F3 was measured by ICP-OES, the contents of several elements in this fraction were generally below the detection limit (Co, Ni, and V) or not measured at all (As, Cd, Pb, and Sn). Diagenetic zonation (as in Fig. 2) and the interval of enhanced terrestrial organic matter input (as in Fig. 5A) are also indicated.

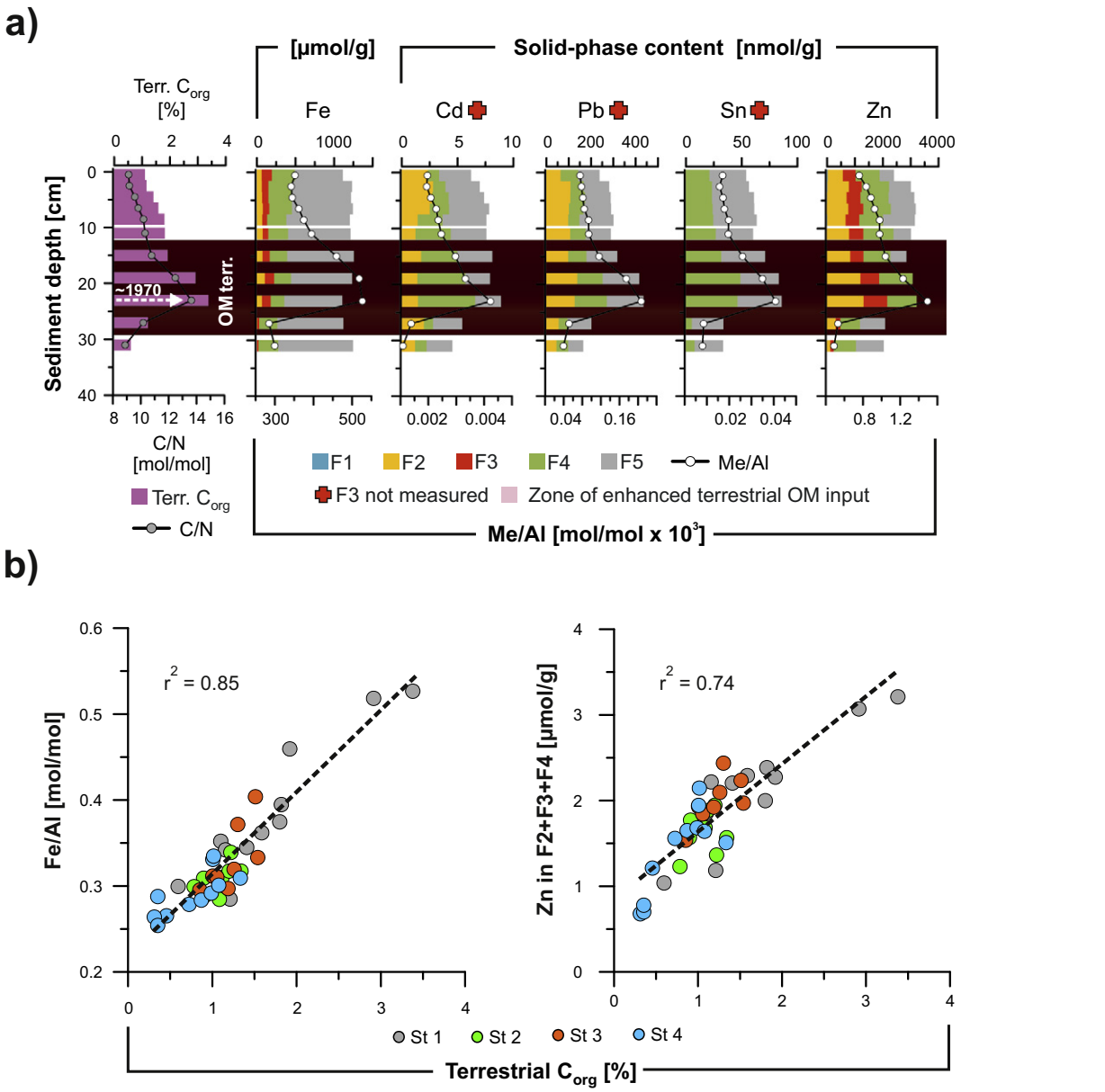

Fig. 8. (A) Downcore variations in C/N ratio, terrestrial C_{org} content, and metal speciation at Station 1. Aluminium-normalized total metal contents (Me/Al) are also shown. (B) Cross plots of Fe/Al ratio and Zn content in fractions F1, F2, and F3 versus terrestrial C_{org}. The interval of enhanced terrestrial organic matter input as in Fig. 5A.

Of concern to our interpretations, however, is the fate of pyrite during the incineration step, since this mineral often provides an important vector for trace metal sequestration in sulfidic sediments (Huerta-Diaz and Morse, 1992; Morse and Luther III, 1999; Scholz and Neumann, 2007), and some studies suggest thermal decomposition or direct oxidation of pyrite around 500 °C (Hu et al., 2006 and references therein). To assess whether the pyrite-bound trace metals dissolved in F4, we can compare the trace metal contents in this fraction with the profile of total solid-phase S, which provides a first-order estimate for pyrite content in the sediments of Pojo Bay (Jilbert et al., 2018). The comparison shows that the trace metals with the strongest reported affinity to pyrite, such as As, Co, Cu and Ni (Huerta-Diaz and Morse, 1992; Morse and Luther III, 1999; Scholz and Neumann, 2007) are generally decoupled from total S (Fig. S2). Therefore, we infer that pyrite is not significantly contributing to the trace metal pool in F4, and that this pool is likely dominated by refractory metal-OM complexes that were not recovered in fractions F1–F3. The pivotal role of OM as a trace metal host in F4 is further supporter by the PCA analysis, where PC1 explains >50% of the total variance in this fraction, effectively dividing the trace metals into two groups largely based on their co-variation with either terrestrial or phytoplankton-derived OM (Fig. 4B).

4.1.5. Fraction 5

The residual fraction F5 was originally suggested to contain trace metals hosted by detrital silicate minerals, refractory sulfides, and potentially by refractory OM (Tessier et al., 1979). The bulk of this trace metal pool is likely derived from the crystal lattice of silicate minerals, (Carral et al., 1995; Heltai et al., 2005), as clearly illustrated by the near 1:1 match between Cr content in F5 and total Al ($r_s = 0.93$, $p < 0.001$). In addition, as opposed to F4, the coupling between total solid-phase S content and trace metals generally typified by a high degree of pyritization (As, Co, Cu, and Ni) in F5 (Figs. 4C and S3; Huerta-Diaz and Morse, 1992; Morse and Luther III, 1999; Scholz and Neumann, 2007) signals that a marked fraction of the F5 pool of these elements is associated with pyrite. In contrast, we find no evidence for coupling between trace metals in F5 and the contents of

phytoplankton-derived or terrestrial C_{org} (Figs. 4C and 7), implying negligible contribution from refractory OM in this fraction.

4.2. Temporal variations in trace metal (Cd, Pb, Sn, and Zn) sequestration driven by atmospheric fallout and terrestrial OM input

Although our study sites are located in the vicinity of the former Koverhar steel factory (Fig. 1b), we find no unambiguous evidence of enhanced trace metal input originating from this local point source. Instead, we infer that the observed temporal variations in the trace metal solid-phase accumulation, specifically the interval of significantly augmented sequestration of Cd, Pb, Sn, and Zn (Fig. 7) reflects a regional signal from the Pojo Bay catchment. Evidence for this is provided by the following observations: (1) the interval of intensified trace metal accumulation is observed consistently throughout the estuary, with decreasing amplitude towards the outer archipelago (cf. Jilbert et al., 2018; Fig. S4); (2) no clear gradient in the solid-phase trace metal content is observed along our study transect away from the factory (Fig. 7); (3) the trace metal contents at the study sites are approximately equal to the typical values along the Finnish coast of the Gulf of Finland (c.f. Vallius, 2009). Accordingly, it was recognized already in the 1970s that the trace metal pollution originating from the Koverhar factory is spread heterogeneously in the adjacent sediments (Luotamo and Luotamo, 1979). Therefore, we henceforth interpret the observed temporal variations in the trace metal input predominantly in the context of regional anthropogenic forcing.

Further clues to the source of enhanced delivery of Cd, Pb, Sn, and Zn can be gleaned from studies of the history of heavy metal pollution in Finnish lakes. The comprehensive studies by Verta et al. (1989) and Mannio et al. (1993) showed that the input of Cd, Pb and Zn (Sn was not included in these studies) to lake sediments in southern Finland is predominantly sourced from long-range atmospheric transport. The human-induced atmospheric heavy metal input peaked in the 1970s due to intensive combustion of fossil fuels and usage of leaded gasoline (Rühling and Tyler, 2001), and the effects of this intensified fallout are consistently recorded both in lake sediments in south-central Finland (Verta et al., 1989; Hakala and Salonen, 2004; Meriläinen et al., 2010) and in coastal sediments off southern Finland (Virtasalo et al., 2014b; Jilbert et al., 2018; Jokinen et al., 2018). The consistency between the records is a manifestation of the large-scale atmospheric fallout pattern that modulates heavy metal sequestration into lake sediments throughout Scandinavia (Skjelkvåle et al., 2001). Furthermore, despite the scarcity of data for Sn content in sediment records of northern Europe, this trace metal is strongly enriched in aerosols (Byrd and Andreae, 1986), being largely derived from anthropogenic sources such as metal smelting and combustion processes (e.g Bjerregaard and Andersen, 2007). Taken together, it is reasonable to assume that the synchronous increases in the total solid-phase content of Cd, Pb, Sn, and Zn were connected to the peak in human-induced atmospheric fallout in the 1970s.

The temporal variations in the accumulation of Cd, Pb, Sn, and Zn sourced from atmospheric fallout appear intimately coupled to terrestrial OM input including the coincident peaks around the 1970s (Figs. 4D, 7 and 8). To explain this linkage, it should be noted that the vast majority of riverine OM input to Finnish estuaries operationally classifies as DOM (Mattsson et al., 2005; Jilbert et al., 2018), which is a mixture of colloidal and truly dissolved material (e.g. Nystrand et al., 2012). Considering the strong affinity of trace metals to DOM, and specifically to humic substances (Benedetti et al., 1996; Leenheer et al., 1998; Yang and van der Berg, 2009), this intimate association suggests that terrestrial OM could provide an important vector for trace metal transport along the land-sea continuum. Accordingly, we posit that concurrently with the intensified atmospheric deposition of these trace metals in Scandinavia in the 1970s (Rühling and Tyler, 2001), their delivery from the catchment soils and lakes to the Pojo Bay estuary was substantially augmented by effective metal-OM complexation (Pokrovsky and Schott, 2002; Huser et al., 2012; Lidman et al., 2014, 2017; Broder and Biester, 2017; Levshina, 2018). Analogously to terrestrial OM, it is likely that these metal-OM complexes are carried in the river water predominantly in dissolved/colloidal form. Potential sources for the accentuated DOM supply in the 1970s include urbanization (Aitkenhead-Peterson et al., 2009; Gücker et al., 2016) as well as intensified land use practices both in agriculture (McTiernan et al., 2001; Mattsson et al., 2005) and forestry (Kortelainen et al., 1997; Laudon et al., 2009; Schelker et al., 2012). In addition to these factors, effluents from pulp and paper milling on the shores of Lohjanjärvi peaked in the 1970s, as evidenced by a pronounced peak in sedimentary resin acids in the south-eastern part of the Lake (Heikkinen, 2000). This implies that large amounts of lignin and other organic compounds derived from paper and pulp industry were discharged to the receiving waters (including Pojo Bay) prior to the establishment of activated sludge plants in the 1980s (Katko et al., 2005). Collectively, we conclude that all these factors combined to induce a pronounced maximum in the input of terrestrial OM to the Pojo Bay in the 1970s.

The enhanced export of DOM in the 1970s in this system implies that intensified human activity outweighed the effects of atmospheric sulfate deposition, which also peaked broadly at the same time (Schöpp et al., 2003) and has been shown to stabilize DOM through proton-induced neutralization of its net charge (Ekström et al., 2011; Evans et al., 2012). Similar overriding effects of land use changes on DOM export are corroborated by the findings of Yu et al. (2015), who observed a substantial increase in DOM input to a nearby boreal estuary in the 1970s due to ditching activities in the catchment.

4.3. Sedimentation mechanisms of terrestrial OM-bound trace metals

In order to explain sediment sequestration of trace metal phases associated with riverine input of metal-OM complexes, a specific mechanism for their conversion to the particulate pool needs to be invoked. Accordingly, we suggest that flocculation caused by an increase in ionic strength is a key process driving sedimentation of the riverine metal-OM complexes upon their entrance to the estuarine brackish water (Boyle et al., 1977; Sholkovitz, 1978; Wells et al., 2000). As DOM flocculates due to cation-induced balancing of the net negative surface charge (Eckert and Sholkovitz, 1976), the trace metals associated with it become passively exposed to this process (Sholkovitz et al., 1978; Stolpe and Hassellöv, 2007; Karbassi et al., 2007; Biati et al., 2010; Samani et al., 2014), whereby the metal-OM complexes are transferred from dissolved (or colloidal) to particulate form. The proposed sedimentation mechanism concurs with the work by Asmala et al. (2014, 2016), which demonstrated effective flocculation of DOM along the salinity gradient in the Pojo Bay estuary. Alongside DOM, another important vector for riverine trace metal input are Fe (oxyhydr) oxides, and especially ferrihydrite, which is a common weathering product of Fe-bearing minerals in boreal regions and efficient trace metal sorbent in the aquatic environment (Raiswell, 2011; Schultz et al., 1987). Ferrihydrite (and the associated trace metals) effectively sorbs to DOM (Eusterhues et al., 2008), but also itself undergoes flocculation in the estuary (Jilbert et al., 2018). Consequently, trace metals in boreal rivers and estuaries are often associated with Fe-rich organo-mineral colloids (Stolpe and Hassellöv, 2007; Wällstedt et al., 2010; Neubauer et al., 2013; Oni et al., 2013).

The expected linkages among riverine input of ferrihydrite, DOM, and trace metals are manifested in the near 1:1 match between terrestrial C_{org} and metal/Al ratios of Cd, Fe, Pb, Sn, and Zn (Fig. 8). Considering that Fe/Al provides a first-order proxy for the input of flocculated material in the sediments of Pojo Bay (Jilbert et al., 2018), this coupling evidences similar pathways of river transport and subsequent flocculation-induced sediment sequestration in the estuary for terrestrial OM, ferrihydrite, Cd, Pb, Sn, and Zn. Although the flocculation processes are generally most intensive in the inner part of the Pojo Bay estuary (Asmala et al., 2014; Jilbert et al., 2018), a substantial fraction of the resulting suspended particulate matter is expected to be

transported towards our study sites in the middle archipelago due to the short residence time of the inner estuary surface waters (Stipa, 1999). Moreover, similarly to the Kalix River estuary in the northernmost Baltic Sea, lateral transport of the flocculated material towards the outer estuary may be enhanced by incorporation into low-density organic-rich aggregates (Gustafsson et al., 2000). Compatible with this, the general decoupling between total solid-phase Al and Cd, Pb, Sn, and Zn (Fig. 4D) signals negligible contribution from suspended siliciclastic material to the flocculation-induced settling of these trace metals.

Based on the sequential extraction, the increase in total solid-phase content of Cd, Pb, Sn, and Zn during the period of accentuated terrestrial OM accumulation around 1970s can be almost exclusively attributed to enhanced sequestration in fractions F2–F4 (Figs. 7 and 8A), which are largely composed of metal-OM complexes as outlined in Section 4.1. This association is also clearly demonstrated in the cross plot of terrestrial C_{org} against Zn in F2–F4 for all measured samples (Fig. 8B), which indicates that the coupling holds consistently throughout the profiles. Furthermore, considering that DOM hosts a heterogeneous mixture of different metal-binding functional groups with highly variable binding affinities (Ghosh and Banerjee, 1997; Warren and Haack, 2001; Jeong et al., 2007), it is not unexpected that terrestrially-derived metal-OM complexes appear to reside in multiple fractions in the sediment. The wide range of lability among the terrestrially-derived metal-OM complexes is also compatible with the preferential removal of humic-like substances from the DOM pool upon flocculation in the estuary (Asmala et al., 2014, 2016), which carry a diverse array of metal-sorbing functional groups (e.g. Yang and van der Berg, 2009; Baran et al., 2019). It is also worth noting that there is element-specific variation in the trace metal speciation associated with the period of enhanced sequestration in the 1970s. For example, while the increase in Zn is largely due to enhanced sequestration in F2 over this interval, Sn uptake exclusively occurs in F4 (Figs. 7 and 8B). These observations collectively concur with the reported differences in the binding strength of Me-OM complexes, not only among different functional groups, but also between different trace metals (Santschi et al., 1997).

4.4. Effects of diagenesis on trace metal burial and speciation

Superimposed on the temporal variations in trace metal input and accumulation, speciation of most of the trace metals studied is affected by early diagenetic processes. In the following, we separately deconvolve the effects of diagenesis on trace metal speciation above and within the SMTZ based on the sequential extraction and pore water data. We specifically focus on the near-surface enrichment in the most mobile fractions, and subsequent increases in the residual trace metal pool within the SMTZ.

4.4.1. Diagenetic processes within the zone of OCR-Fe-Mn

As outlined in Section 4.1 the most plausible host phases for the observed near-surface enrichments in F2 (Cd, Co, Fe, Mn, Ni, Zn) and F3 (Cu, Fe, Mn) comprise labile metal-OM complexes and Fe—Mn (oxyhydr)oxides (Table 2). Below the near-surface enrichment, the generally downward decreasing trace metal content in F2 and F3 (Fig. 7) likely denotes trace metal dissolution from these relatively labile phases upon microbial OM degradation and associated dissimilatory reduction of Fe—Mn (oxyhydr)oxides (organo-clastic reduction) (Shaw et al., 1990; Tankere-Muller et al., 2007; Santos-Echeandia et al., 2009; Olson et al., 2017). Indeed, trace metal delivery to surface sediments is often ascribed to particulate shuttling, whereby these phases act as prime metal carrier phases across the SWI (Algeo and Tribovillard, 2009; Little et al., 2015). This shuttling is most likely catalyzed by flocculation processes in the surface waters of the estuary, which convert dissolved and colloidal constituents to particulate form (Dagg et al., 2004).

The pore water profiles are congruent with the inferred initial trace metal sequestration by labile OM and Fe—Mn (oxyhydr)oxides and subsequent dissolution in the surface sediments. Specifically, this pattern of particulate shuttling is supported by the elevated trace metal concentrations in the dissolved pool within the zone OCR-Fe-Mn (Figs. 2 and 3). Moreover, we note that the bottom water trace metal concentrations generally exceed the expected salinity-normalized levels as well as the concentrations in the local stream waters by 1–3 orders of magnitude (Table 3). Such bottom water enrichments likely reflect effective diagenetic recycling of the most labile trace metal carrier phases above the SMTZ (Ingri et al., 2014), which often results in diffusive efflux of trace metals to the bottom waters in estuarine and coastal settings (e.g. Emerson et al., 1984; Jones and Turki, 1997; Emili et al., 2016). On the other hand, trace metal accumulation in the pore waters within the zone of OCR-Fe-Mn also induces a downward diffusive flux towards the SMTZ.

4.4.2. Diagenetic processes within the SMTZ

At the transition to the SMTZ a sink-switch from F2 and F3 to the refractory fractions F4 and F5 is observed especially for As, Cd, Co, Cu and Ni (Fig. 7). As a result of this diagenetic redistribution, As, Co, Cu, and Ni display a downward increase in F5 within the SMTZ, while Cd appears to undergo a sink-switch from F2 to F4. This contrast in the ultimate host phases likely denotes different mechanisms of incorporation into insoluble sulfides, as outlined below.

We infer that the sink-switching of Cd from F2 to F4 within the SMTZ signals dissolution of Cd-OM complexes and subsequent solid-phase uptake via CdS precipitation upon exposure to dissolved sulfide (Rosenthal et al., 1995; Gobeil et al., 1997; Audry et al., 2006). Accordingly, due to very low solubility and fast precipitation kinetics of CdS, Cd is efficiently sequestered in this phase under sulfidic conditions, resulting in negligible uptake into pyrite (Huerta-Diaz and Morse, 1992; Morse and Luther III, 1999; Burton et al., 2006a). Furthermore, although AVS phases are expected to primarily reside in fractions F2 and F3 (Section 4.1; Table 2), CdS exhibits exceptional stability over a wide pH range (Kersten, 2002), implying that this phase could remain immobile over the extraction steps 1–3. However, we note that these effects of diagenetic Cd redistribution are partly masked by the temporal variability in riverine trace metal input associated with metal-OM complexes, which has substantially modulated the content of Cd in fractions F2 and F4 (Section 4.2).

In contrast to Cd, we suggest that the gradual downward increase in As, Co, Cu, and Ni in F5 within the SMTZ reflects their progressive incorporation into pyrite, which is consistent with previous studies on trace metal sequestration in sulfide-bearing sediments (Huerta-Diaz and Morse, 1992; Scholz and Neumann, 2007; Morgan et al., 2012). The sink-switch from labile phases to pyrite is most prominent at Station 2, where a marked increase in As, Co, Cu, and Ni contents in F5 occurs at the expense of fractions F2 (As, Co, Ni) and F3 (Cu) at the transition to SMTZ (Fig. 7). Importantly, this conversion coincides with the depth interval of effective pyrite formation as implied by a synchronous increase in solid-phase S content and a decrease in Fe/S ratio (Fig. 5b). These observations conform to the relatively slow reaction kinetics of As, Co, Cu, and Ni for monosulfide precipitation, which drives their preferential incorporation into pyrite upon exposure to dissolved sulfide (Huerta-Diaz and Morse, 1992; Morse and Luther III, 1999; Sternbeck et al., 2000; Müller, 2002; Oueslati et al., 2018). Among the studied trace metals, the diagenetic uptake into pyrite is expected to be most effective for As (Huerta-Diaz and Morse, 1992), concurring with the particularly strong coupling between As in F5 and total S (Fig. S3).

The presence of pyrite-bound trace metals in F5 signals particularly strong association between the trace metals and the host phase. Indeed, recent investigations have shown that pyrite hosts trace metals either within its crystal structure (e.g. Ni, Co) or as sulfide micro- or nanoinclusions (e.g. As, Cu; Large et al., 2009, 2014; Deditius et al., 2011; Gregory et al., 2015). Consistent with these suggestions, strong bonding between trace metals and pyrite has been explained by initial adsorption onto surface of freshly-formed pyrite, followed by

Table 3
Trace metal concentrations in seawater (salinity-normalized) and local streams. All values are given in nM.

Medium	As	Cd	Co	Cr	Cu	Ni	Pb	Sn	V	Zn
Bottom water[a]	33.4	0.5	2.2	33.5	76.5	52.3	3.3	12.9	37.2	4560
Sea water (salinity-normalized)[b]	5.1	0.1	0.005	1.1	0.3	1.4	<0.001	<0.001	3.4	1.0
Local stream waters[c]	10.7	0.2	5.1	4.8	23.6	17.0	1.1		13.8	58

[a] Average of the measured bottom water concentrations in this study.
[b] Depth-averaged ocean concentrations (Sarmiento and Gruber, 2006) normalized to ambient salinity.
[c] Local stream water concentrations reported in Lahermo et al. (1996).

incorporation and protection during successive diagenetic crystal growth (Schoonen, 2004; Scholz and Neumann, 2007). In this context, our findings add to the existing evidence that pyrite constitutes an important permanent sink for As, Co, Cu, and Ni in sulfide-bearing sediments.

Despite the incorporation of As, Cd, Co, Cu, and Ni into insoluble sulfides, the pore water data points to inefficient removal of these trace metals from the pore waters within the SMTZ (Fig. 3). Similar trace metal behavior has been reported from other sulfidic settings, where unexpectedly high trace metal solubility at non-negligible dissolved sulfide levels has been linked to the formation of dissolved metal-polysulfide complexes (Gobeil et al., 1987; Huerta-Diaz et al., 1998; Wang and Tessier, 2009; Dang et al., 2015), metal binding with DOM (Gobeil et al., 1987; Charriau et al., 2011; Lourino-Cabana et al., 2014), and to metal-sulfide-DOM ternary interactions (Hoffmann et al., 2012). We do not have data for pore water DOM, but to a first-order approximation, we assume that its concentration broadly follows the NH_4^+ and HPO_4^{2-} profiles, hence increasing progressively with depth upon degradation of OM (e.g. Burdige and Zheng, 1998), with the steepest gradient at the transition to the SMTZ (Brodecka-Goluch and Łukawska-Matuszewska, 2018). The implied downward increase in the availability of binding sites provided by DOM potentially stimulates formation of soluble metal-DOM complexes in the pore waters within the SMTZ (Charriau et al., 2011; Rigaud et al., 2013; Dang et al., 2015; Olson et al., 2017). Specifically, formation of strong organic ligands, such as thiols upon interaction between organic molecules and dissolved sulfide (Zonneveld et al., 2010) could catalyze trace metal mobilization within the SMTZ (Huerta-Diaz et al., 1998). This concurs with the findings of Charriau et al. (2011) who used a combination of sequential extraction experiments and thermodynamic equilibrium calculations to demonstrate that despite the extremely fast MeS precipitation kinetics of Cd, Pb, and Zn, metal-DOM interactions may retain these trace metals dissolved in the pore water in the presence of dissolved sulfide. Finally, we note that alongside DOM-induced increase in trace metal solubility, deep dissolution of Fe—Mn (oxyhydr)oxides coupled to anaerobic oxidation of methane (Beal et al., 2009; Egger et al., 2015) or persistent organo-clastic reduction (Jilbert et al., 2018) may increase the dissolved trace metal pool within the SMTZ, as suggested by the progressive downward increase in pore water Mn concentration (Fig. 2).

4.4.3. Trace metal pools unaffected by diagenesis

Of the studied trace metals, the speciation of Cr and V remains largely unaffected throughout the solid-phase profiles (Fig. 7). Both of these elements principally reside in the residual fraction (Fig. 6), being in agreement with previous studies on sedimentary trace metal speciation in other coastal settings (Yuan et al., 2004; Passos et al., 2010; Yu et al., 2014; Emili et al., 2016; Bastami et al., 2017). The largely inert behavior of Cr during diagenesis is consistent with its structural and electronic incompatibility with pyrite and the generally weak ability of Cr^{3+} to form insoluble sulfides (Morse and Luther III, 1999; Kim et al., 2001; Burton et al., 2006a). Instead, Cr readily substitutes for Fe and Mg within the crystal lattice of clay and ferromagnesian minerals (e.g. Francois, 1988; Hild and Brumsack, 1998). Similarly to Cr, V is not effectively scavenged from aqueous solutions by Fe-sulfides (Algeo and Maynard, 2004), while it readily replaces Al in octahedral sites of clay minerals (Breit and Wanty, 1991). Hence, we infer that the total solid-phase Cr and V contents in the studies sediments are principally dictated by the input of siliciclastic material, as illustrated by their strong correlation with total Al ($r_s = 0.90$, $p < 0.001$ and $r_s = 0.80$, $p < 0.001$, respectively). However, we note that the increasing concentrations of dissolved Cr and V at the transition to the SMTZ (Fig. 3), suggest subtle diagenetic activity for these elements. Analogously to the other trace metals (Section 4.4.2), this mobilization within the SMTZ could be related to complexation with organic and/or sulfide ligands, or deep dissolution of Fe—Mn (oxyhydr)oxides upon to anaerobic oxidation of methane or persistent organo-clastic reduction.

Alongside Cr and V, refractory metal-OM complexes (F4) constitute a quantitatively important trace metal pool that remains largely unaffected by diagenetic processes. Excluding the diagenetic increase in Cd (Section 4.4.2), this is manifested in the markedly constant trace metal levels in F4 both above and across the transition to the SMTZ (Figs. 6 and 7). Considering that the organic ligands that host the trace metals in refractory metal-OM complexes in F4 likely comprise a mixture of functional groups derived from both terrestrial and autochthonous sources (Bianchi et al., 2004), it is remarkable that Cd, Pb, Sn, and Zn in this fraction are specifically coupled to terrestrial C_{org} (Fig. 4B). As such, sequestration of these trace metals into F4 appear to capture changes in terrestrial OM input despite the effects of diagenesis.

5. Implications and conclusions

Despite the wide recognition pertaining to the strong affinity of trace metals to humic substances in the aquatic environment (e.g. Reuter and Perdue, 1977; Mantoura et al., 1978; Schnitzer and Kerndorf, 1981; Davis, 1984; Benedetti et al., 1996; Leenheer et al., 1998; Tipping et al., 1998; Weng et al., 2002; Gustafsson et al., 2003; Yang and van der Berg, 2009; Baran et al., 2019) and to the importance of metal-OM complexes in land-to-sea transfer of trace metals (e.g. Pokrovsky and Schott, 2002; Stolpe and Hassellöv, 2007; Wällstedt et al., 2010; Oni et al., 2013; Stolpe et al., 2013; Lidman et al., 2014, 2017; Wang et al., 2017; Levshina, 2018), only a few previous studies explicitly attribute trace metal accumulation in estuarine sediments to terrestrial OM delivery (Fukushima et al., 1992; Krupadam et al., 2003; De la Rosa et al., 2011; Yu et al., 2014; Chakrabotry et al., 2016). In this context, an important implication of this study is that terrestrial metal-OM complexes not only play a key role in trace metal delivery to estuarine waters, but could also exert a first-order control on trace metal sequestration in coastal sediments. We suggest that this persistent association between terrestrial OM and trace metals from hinterland freshwater environments to estuarine sediments may be more common than previously thought, as evidenced by the generally observed non-conservative removal of dissolved/colloidal terrestrial OM and associated trace metals into particulate form through flocculation and aggregation processes during estuarine mixing (Sholkovitz, 1978; Wells et al., 2000; Turner et al., 2002; Stolpe and Hassellöv, 2007; Biati et al., 2010; Samani et al., 2014; Heidari, 2019). Such an oversight could simply result from the fact that most studies on trace metal sequestration in estuarine settings only consider the bulk sedimentary OM pool and neglect source apportionment (Wassermann et al., 1998; De la Rosa et al., 2011).

Another key finding of this study is that the sedimentation of terrestrially-derived metal-OM complexes fundamentally affects

diagenetic processing of trace metals. The trace metal pool associated with a relatively low binding strength is effectively recycled in the surface sediments above the SMTZ, with the ultimate fate of either efflux to the bottom waters or permanent burial upon downward diffusion and subsequent sequestration into insoluble sulfide phases. By contrast, a major fraction of the trace metal input associated with terrestrial OM enters the estuary and the sediments in the form of particularly refractory metal-complexes (F4), which appear to undergo negligible diagenetic mobilization. Combined, these findings imply that although metal-OM complexation potentially augments land-to-sea transport of anthropogenically-sourced trace metals, a substantial fraction of this trace metal pool is permanently buried in the sediment. As such, flocculation-induced sedimentation of terrestrial metal-OM complexes in these estuarine sediments constitutes a substantial long-term sink for trace metals, thereby serving as a potential buffer against anthropogenic input from the catchment.

Finally, our results suggest that despite the effects of diagenetic redistribution, the ultimate sediment sequestration of Pb, Cd, Sn, and Zn in the Pojo Bay estuary is likely proportional to the anthropogenic loading from the hinterland. The current trace metal levels in these sediments are on a declining trajectory, but yet remain elevated above the geochemical background, as evidenced by the substantially lower contents at the base of the studied cores (Fig. 7). However, considering that the least reactive fractions F4 and F5 dominate the sedimentary trace metal pools, the modern trace metal contents are not expected to pose substantial environmental risks.

Funding

This work was funded by the Academy of Finland [grant numbers 278827, 304006, 312495, 317684, 319956].

Author contribution

Sami Jokinen: Writing – original draft, Formal analysis, Conceptualization, Investigation. **Tom Jilbert:** Writing – review and editing, Conceptualization, Methodology, Supervision, Funding acquisition, Investigation. **Rosa Tiihonen-Filppula:** Investigation, Methodology, Writing – review and editing. **Karoliina Koho:** Writing – review and editing, Conceptualization, Supervision, Funding acquisition, Investigation.

Declaration of competing interest

The authors declare that they have no known competing financial interests or personal relationships that could have appeared to influence the work reported in this paper.

Acknowledgements

We would like to acknowledge Tvärminne Zoological Station for their valuable support in facilitating field work and laboratory analyses. We specifically thank Alf Norkko, Joanna Norkko, Göran Lundberg, Veijo Kinnunen, Tero Mustonen, Hanna Halonen, Jaana Koistinen, Antti Nevalainen, and Mervi Sjöblom. We also acknowledge Iines Salonen, Myrsini Chronopoulou, and Pirita Anttila for their valuable help in the field work. Utrecht University GeoLab, especially Helen de Waard, is thanked for performing the ICP-MS and ICP-OES analyses. Joonas Virtasalo is thanked for insightful comments on the manuscript. This study has utilized research infrastructure facilities provided by FINMARI (Finnish Marine Research Infrastructure network).

Appendix A. Supplementary data

Supplementary data to this article can be found online at https://doi.org/10.1016/j.scitotenv.2020.137047.

References

Aitkenhead-Peterson, J.A., Steele, M.K., Nahar, N., Santhy, K., 2009. Dissolved organic carbon and nitrogen in urban and rural watersheds of south-central Texas: land use and land management influences. Biogeochemistry 96 (1–3), 119–129. https://doi.org/10.1007/s10533-009-9348-2.

Algeo, T.J., Maynard, J.B., 2004. Trace-element behavior and redox facies in core shales of Upper Pennsylvanian Kansas-type cyclothems. Chem. Geol. 206 (3–4), 289–318. https://doi.org/10.1016/j.chemgeo.2003.12.009.

Algeo, T.J., Tribovillard, N., 2009. Environmental analysis of paleoceanographic systems based on molybdenum–uranium covariation. Chem. Geol. 268 (3–4), 211–225. https://doi.org/10.1016/j.chemgeo.2009.09.001.

Allen, H.E., Hall, R.H., Brisbin, T.D., 1980. Metal speciation. Effects of aquatic toxicity. Environmental Science & Technology 14 (4), 441–443. https://doi.org/10.1021/es60164a002.

Amato, E.D., Simpson, S.L., Belzunce-Segarra, M.J., Jarolimek, C.V., Jolley, D.F., 2015. Metal fluxes from porewaters and labile sediment phases for predicting metal exposure and bioaccumulation in benthic invertebrates. Environmental Science & Technology 49 (24), 14204–14212. https://doi.org/10.1021/acs.est.5b03655.

Anderson, B.J., Jenne, E.A., 1970. Free-iron and -manganese oxide content of reference clays. Soil Sci. 109 (3), 163–169.

Asmala, E., Bowers, D.G., Autio, R., Kaartokallio, H., Thomas, D.N., 2014. Qualitative changes of riverine dissolved organic matter at low salinities due to flocculation. Journal of Geophysical Research: Biogeosciences 119 (10), 1919–1933. https://doi.org/10.1002/2014JG002722.

Asmala, E., Kaartokallio, H., Carstensen, J., Thomas, D.N., 2016. Variation in riverine inputs affect dissolved organic matter characteristics throughout the estuarine gradient. Front. Mar. Sci. 2 (125). https://doi.org/10.3389/fmars.2015.00125.

Audry, S., Blanc, G., Schäfer, J., Chaillou, G., Robert, S., 2006. Early diagenesis of trace metals (Cd, Cu, Co, Ni, U, Mo, and V) in the freshwater reaches of a macrotidal estuary. Geochim. Cosmochim. Acta 70 (9), 2264–2282. https://doi.org/10.1016/j.gca.2006.02.001.

Ball, D.F., 1964. Loss-on-ignition as an estimate of organic matter and organic carbon in non-calcareous soils. J. Soil Sci. 15 (1), 84–92. https://doi.org/10.1111/j.1365-2389.1964.tb00247.x.

Baran, A., Mierzwa-Hersztek, M., Gondek, K., Tarnawski, M., Szara, M., Gorczyca, O., Koniarz, T., 2019. The influence of the quantity and quality of sediment organic matter on the potential mobility and toxicity of trace elements in bottom sediment. Environ. Geochem. Health 41 (6), 2893–2910. https://doi.org/10.1007/s10653-019-00359-7.

Bastami, K.D., Neyestani, M.R., Esmaeilzadeh, M., Haghparast, S., Alavi, C., Fathi, S., Nourbakhsh, S., Shirzadi, E.A., Parhizgar, R., 2017. Geochemical speciation, bioavailability and source identification of selected metals in surface sediments of the Southern Caspian Sea. Mar. Pollut. Bull. 114 (2), 1014–1023. https://doi.org/10.1016/j.marpolbul.2016.11.025.

Beal, E.J., House, C.H., Orphan, V.J., 2009. Manganese and iron dependent marine methane oxidation. Science 325, 184–187. https://doi.org/10.1126/science.1169984.

Benedetti, M.F., van Riemsdijk, W.H., Koopal, L.K., Kinniburgh, D.G., Gooddy, D.C., Milne, C.J., 1996. Metal ion binding by natural organic matter: from the model to the field. Geochim. Cosmochim. Acta 60 (14), 2503–2513. https://doi.org/10.1016/0016-7037(96)00113-5.

Bianchi, T.S., Filley, T., Dria, K., Hatcher, P.G., 2004. Temporal variability in sources of dissolved organic carbon in the lower Mississippi river. Geochim. Cosmochim. Acta 68 (5), 959–967. https://doi.org/10.1016/j.gca.2003.07.011.

Biati, A., Karbassi, A.R., Hassani, A.H., Monavari, S.M., Moattar, F., 2010. Role of metal species in flocculation rate during estuarine mixing. International Journal of Environmental Science & Technology 7 (2), 327–336. https://doi.org/10.1007/BF03326142.

Bjerregaard, P., Andersen, 2007. Ecotoxicology of metals — sources, transport, and effects in the ecosystem. In: Nordberg, G.F., Fowler, B.A., Nordberg, M., Friberg, L. (Eds.), Handbook on the Toxicology of Metals. Academic Press, San Diego, pp. 251–280.

Bonaglia, S., Bartoli, M., Gunnarsson, J.S., Rahm, L., Raymond, C., Svensson, O., Yekta, S., Brüchert, V., 2013. Effect of reoxygenation and Marenzelleria spp. bioturbation on Balti Sea sediment metabolism. Mar. Ecol. Prog. Ser. 482, 43–55. https://doi.org/10.3354/meps10232.

Bordas, F., Bourg, A.C.M., 1998. A critical evaluation of sample pretreatment for storage of contaminated sediments to be investigated for the potential mobility of their heavy metal load. Water Air Soil Pollut. 103 (1–4), 137–149. https://doi.org/10.1023/A:1004952608950.

Boyle, E.A., Edmond, J.M., Sholkovitz, E.R., 1977. The mechanism of iron removal in estuaries. Geochim. Cosmochim. Acta 41 (9), 1313–1324. https://doi.org/10.1016/0016-7037(77)90075-8.

Breit, G.N., Wanty, R.B., 1991. Vanadium accumulation in carbonaceous rocks: a review of geochemical controls during deposition and diagenesis. Chem. Geol. 91 (2), 83–97. https://doi.org/10.1016/0009-2541(91)90083-4.

Brodecka-Goluch, A., Łukawska-Matuszewska, K., 2018. Porewater dissolved organic and inorganic carbon in relation to methane occurrence in sediments of the Gdańsk Basin (southern Baltic Sea). Continental Shel Research 168, 11–20. https://doi.org/10.1016/j.csr.2018.08.008.

Broder, T., Biester, H., 2017. Linking major and trace element concentrations in a headwater stream to DOC release and hydrologic conditions in a bog and peaty riparian zone. Appl. Geochem. 87, 188–201. https://doi.org/10.1016/j.apgeochem.2017.11.003.

Burdige, D.J., Zheng, S., 1998. The biogeochemical cycling of dissolved organic nitrogen in estuarine sediments. Limnol. Oceanogr. 43 (8), 1769–1813. https://doi.org/10.4319/lo.1998.43.8.1796.

Burton, E.D., Phillips, I.R., Hawker, D.W., 2005. Geochemical partitioning of copper, lead, and zinc in benthic, estuarine sediment profiles. J. Environ. Qual. 34 (1), 263–273. https://doi.org/10.2134/jeq2005.0263.

Burton, E.D., Bush, R.T., Sullivan, L.A., 2006a. Fractionation and extractability of sulfur, iron and trace elements in sulfidic sediments. Chemosphere 64 (8), 1421–1428. https://doi.org/10.1016/j.chemosphere.2005.12.003.

Burton, E.D., Phillips, I.R., Hawker, D.W., 2006b. Factors controlling the geochemical partitioning of trace metals in estuarine sediments. Soil & Sediment Contamination 15, 253–276. https://doi.org/10.1080/15320380600646290.

Burton, E.D., Sullivan, L.A., Bush, R.T., Johnston, S.G., Keene, A.F., 2008. A simple and inexpensive chromium-reducible sulfur method for acid-sulfate soils. Appl. Geochem. 23 (9), 2759–2766. https://doi.org/10.1016/j.apgeochem.2008.07.007.

Byrd, J.T., Andreae, M.O., 1986. Concentrations and fluxes of tin in aerosols and rain. Atmos. Environ. 20 (5), 931–939. https://doi.org/10.1016/0004-6981(86)90277-5.

Callender, E., 2005. Heavy metals in the environment – historical trends. In: Lollar, B.S., Holland, H.D., Turekian, K.K. (Eds.), Environmental Geochemistry. Treatise on Geochemistry. Elsevier-Pergamon, Oxford, pp. 67–106.

Canfield, D.E., Jørgensen, B.B., Fossing, H., Glud, R., Gundersen, J., Ramsing, N.B., Thamdrup, B., Hansen, J.W., Nielsen, L.-P., Hall, P.O.J., 1993. Pathways of organic carbon oxidation in three continental margin sediments. Mar. Geol. 113 (1–2), 27–40. https://doi.org/10.1016/0025-3227(93)90147-N.

Canuto, F.A.B., Garcia, C.A.B., Alves, J.P.H., Passos, E.A., 2013. Mobility and ecological risk assessment of trace metals in polluted estuarine sediments using a sequential extraction scheme. Environ. Monit. Assess. 185 (7), 6173–6185. https://doi.org/10.1007/s10661-012-3015-0.

Carral, E., Villares, R., Puente, X., Carballeira, A., 1995. Influence of watershed lithology on heavy metal levels in estuarine sediments and organisms in Galicia (North-West Spain). Mar. Pollut. Bull. 30 (9), 604–608. https://doi.org/10.1016/0025-326X(95)00017-H.

Chakrabotry, P., Chakrabotry, S., Vudamala, K., Sarkar, A., Nath, N., 2016. Partitioning of metals in different binding phases of tropical estuarine sediments: importance of metal chemistry. Environ. Sci. Pollut. Res. 23 (4), 3450–3462. https://doi.org/10.1007/s11356-015-5475-6.

Chao, T.T., 1972. Selective dissolution of manganese oxides from soils and sediments with acidified hydroxylamine hydrochloride. Soil Sci. Soc. Am. Proc. 36, 764–768. https://doi.org/10.2136/sssaj1972.03615995003600050024x.

Charriau, A., Lesven, L., Gao, Y., Leermakers, M., Bayens, W., ouddane, B., Billon, G., 2011. Trace metal behaviour in riverine sediments: role of organic matter and sulfides. Appl. Geochem. 26 (1), 80–90. https://doi.org/10.1016/j.apgeochem.2010.11.005.

Cline, J., 1969. Spectrophotometric determination of hydrogen sulfide in natural waters. Limnol. Oceanogr. 14 (3), 454–458. https://doi.org/10.4319/lo.1969.14.3.0454.

Cooper, D.G., Morse, J.W., 1998. Extractability of metal sulfide minerals in acidic solutions: application to environmental studies of trace metal contamination within anoxic sediments. Environmental Science & Technology 32 (8), 1076–1078. https://doi.org/10.1021/es970415t.

Cornwell, J.C., Morse, J.W., 1987. The characterization of iron sulfide minerals in anoxic marine sediments. Mar. Chem. 22 (2–4), 193–206. https://doi.org/10.1016/0304-4203(87)90008-9.

Dagg, M., Benner, R., Lohrenz, S., Lawrence, D., 2004. Transformation of dissolved and particulate materials on continental shelves influenced by large rivers: plume processes. Cont. Shelf Res. 24 (7–8), 833–858. https://doi.org/10.1016/j.csr.2004.02.003.

Dang, D.H., Lenoble, V., Durrieu, G., Omanovic, D., Mullot, J.-U., Mounier, S., Garnier, C., 2015. Seasonal variations of coastal sedimentary trace metals cycling: insight on the effect of manganese and iron (oxy)hydroxides, sulphide and organic matter. Mar. Pollut. Bull. 92, 113–124. https://doi.org/10.1016/j.marpolbul.2014.12.048.

Dassenakis, M., Scoullos, M., Gaitis, A., 1997. Trace metals transport and behaviour in the Mediterranean estuary of Acheloos River. Mar. Pollut. Bull. 34 (2), 103–111. https://doi.org/10.1016/S0025-326X(96)00062-8.

Davis, J.A., 1984. Complexation of trace metals by adsorbed natural organic matter. Geochim. Cosmochim. Acta 48 (4), 679–691. https://doi.org/10.1016/0016-7037(84)90095-4.

De la Rosa, J.M., Santos, M., Araújo, M.F., 2011. Metal binding by humic acids in recent sediments from the SW Iberian coastal area. Estuar. Coast. Shelf Sci. 93 (4), 478–485. https://doi.org/10.1016/j.ecss.2011.05.029.

Deditius, A.P., Utsunomiya, S., Reich, M., Kesler, S.E., Ewing, R.C., Hough, R., Walshe, J., 2011. Trace metal nanoparticles in pyrite. Ore Geol. Rev. 42 (1), 32–46. https://doi.org/10.1016/j.oregeorev.2011.03.003.

Eckert, J., Sholkovitz, E.R., 1976. The flocculation of iron, aluminium and humates from river water by electrolytes. Geochim. Cosmochim. Acta 40 (7), 847–848. https://doi.org/10.1016/0016-7037(76)90036-3.

Edelman, N., 1949. Structural history of the eastern part of the Gullkrona Basin, SW-Finland. Bulletin de la Commission géologique de Finlande 148, 1–48.

Egger, M., Rasigraf, O., Sapart, C.J., Jilbert, T., Jetten, M.S.M., Rockmann, T., van der Veen, C., Banda, N., Kartal, B., Ettwig, K.F., Slomp, C.P., 2015. Iron-mediated anaerobic oxidation of methane in brackish coastal sediments. Environmental Science & Technology 49, 277–283. https://doi.org/10.1021/es503663z.

Ekström, S.M., Kritzberg, E.S., Kleja, D.B., Larsson, N., Nilsson, P.A., Graneli, W., Bergkvist, B., 2011. Effect of acid deposition on quantity and quality of dissolved organic matter in soil-water. Environmental Science & Technology 45 (11), 4733–4739. https://doi.org/10.1021/es104126f.

Elderfield, H., Hepworth, A., 1975. Diagenesis, metals and pollution in estuaries. Mar. Pollut. Bull. 6 (6), 85–87. https://doi.org/10.1016/0025-326X(75)90149-6.

Emerson, S., Jahnke, R., Heggie, D., 1984. Sediment-water exchange in shallow water estuarine sediments. J. Mar. Res. 42, 709–730.

Emili, A., Acquavita, A., Covelli, S., Spada, L., Di Leo, A., Giandomenico, S., Cardellicchio, N., 2016. Mobility of heavy metals from polluted sediments of a semi-enclosde basin: in situ benthic chamber experiments in Taranto's Mar Piccolo (Ionian Sea, Southern Italy). Environ. Sci. Pollut. Res. 23 (13), 12582–12595. https://doi.org/10.1007/s11356-015-5281-1.

Eusterhues, K., Wagner, F.E., Häusler, W., Hanzlik, M., Knickers, H., Totsche, K.U., Kögel-Knabner, I., Schwertmann, U., 2008. Characterization of ferrihydrite-soil organic matter coprecipitates by X-ray diffraction and Mössbauer Spectroscopy. Environmental Science & Technology 42 (21), 7891–7897. https://doi.org/10.1021/es800881w.

Evans, C.D., Jones, T.G., Burdem, A., Ostle, N., Zieliński, P., Cooper, M.D.A., Peacock, M., Clark, J.M., Oulehle, F., Cooper, D., Freeman, C., 2012. Acidity controls on dissolved organic carbon mobility in organic soils. Glob. Chang. Biol. 18 (11), 3317–3331. https://doi.org/10.1111/j.1365-2486.2012.02794.x.

Francois, R., 1988. A study on the regulation of the concentrations of some trace metals (Rb, Sr, Zn, Pb, Cu, V, Cr, Ni, Mn and Mo) in Saanich Inlet Sediments, British Columbia, Canada. Mar. Geol. 83 (1–4), 285–308. https://doi.org/10.1016/0025-3227(88)90063-1.

Froelich, P.N., Klinkhammer, G.P., Bender, M.L., Luedtke, N.A., Heath, G.R., Cullen, D., Dauphin, P., 1979. Early oxidation of organic matter in pelagic organic sediments of the eastern equatorial Atlantic: suboxic diagenesis. Geochim. Cosmochim. Acta 43 (7), 1075–1090. https://doi.org/10.1016/0016-7037(79)90095-4.

Fukushima, K., Saino, T., Kodama, Y., 1992. Trace metal contamination in Tokyo Bay, Japan. Sci. Total Environ. 125, 373–389. https://doi.org/10.1016/0048-9697(92)90402-E.

Gao, X., Zhou, F., Chen, C.-T.A., 2014. Pollution status of the Bohai Sea: an overview of the environmental quality assessment related trace metals. Environ. Int. 62, 12–30. https://doi.org/10.1016/j.envint.2013.09.019.

Ghosh, R., Banerjee, D.K., 1997. Complexation of trace metals with humic acids from soil, sediment and sewage. Chemical Speciation & Bioavailability 9 (1), 15–19. https://doi.org/10.1080/09542299.1997.11083279.

Gibbs, R.J., 1986. Segregation of metals by coagulation in estuaries. Mar. Chem. 18 (2–4), 149–159. https://doi.org/10.1016/0304-4203(86)90004-6.

Gleyzes, C., Tellier, S., Astruc, M., 2002. Fractionation studies of trace elements in contaminated soils and sediments: a review of sequential extraction procedures. Trends Anal. Chem. 21 (6–7), 451–467. https://doi.org/10.1016/S0165-9936(02)00603-9.

Gobeil, C., Silverberg, N., Sundby, B., Cossa, D., 1987. Cadmium diagenesis in Laurentian Trough sediments. Geochim. Cosmochim. Acta 51 (3), 589–596. https://doi.org/10.1016/0016-7037(87)90071-8.

Gobeil, C., Macdonald, R.W., Sundby, B., 1997. Diagenetic separation of cadmium and manganese in suboxic continental margin sediments. Geochim. Cosmochim. Acta 61 (21), 4647–4654. https://doi.org/10.1016/S0016-7037(97)00255-X.

Goñi, M., Teixeira, M., Perkey, D., 2003. Sources and distribution of organic matter in a river dominated estuary (Winyah Bay, SC, USA). Estuarine and Coastal Shelf Science 57 (5–6), 1023–1048. https://doi.org/10.1016/S0272-7714(03)00008-8.

Gregory, D.D., Large, R.R., Halpin, J.A., Baturina, E.L., Lyons, T.W., Wu, S., Danyushevsky, L., Sack, P.J., Chappaz, A., Maslennikov, V.V., Bull, S.W., 2015. Trace element content of sedimentary pyrite in black shales. Econ. Geol. 110 (6), 1389–1410. https://doi.org/10.2113/econgeo.110.6.1389.

Gücker, B., Silva, R.C.S., Graeber, D., Monteiro, J.A.F., Boëchat, I.G., 2016. Urbanization and agriculture increase exports and differentially alter elemental stoichiometry of dissolved organic matter (DOM) from tropical catchments. Sci. Total Environ. 550, 785–792. https://doi.org/10.1016/j.scitotenv.2016.01.158.

Gustafsson, Ö., Widerlund, A., Andersson, P.S., Ingri, J., Roos, P., Ledin, A., 2000. Colloid dynamics and transport of major elements through a boreal river – brackish bay mixing zone. Mar. Chem. 71 (1), 1–21. https://doi.org/10.1016/S0304-4203(00)00035-9.

Gustafsson, J.P., Pechová, P., Bergren, D., 2003. Modeling metal binding to soils: the role of natural organic matter. Environmental Science & Technology 37 (12), 2767–2774. https://doi.org/10.1021/es026249t.

Hakala, A., Salonen, V.-P., 2004. The history of airborne lead and other heavy metals as revealed from sediments of Lake Vähä-Pitkusta, SW Finland. Bull. Geol. Soc. Finl. 76 (1–2), 19–30. https://doi.org/10.17741/bgsf/76.1-2.002.

Hassellöv, M., von der Kammer, F., 2008. Iron oxides as geochemical nanovectors for metal transport in soil-river systems. Elements 4 (6), 401–406. https://doi.org/10.2113/gselements.4.6.401.

Heidari, M., 2019. Role of natural flocculation in eliminating toxic metals. Arch. Environ. Contam. Toxicol. 76 (3), 366–374. https://doi.org/10.1007/s00244-019-00597-x.

Heikkinen, P., 2000. Paperitehtaan jätevesikuormituksen ympäristövaikutukset – sedimenttitutkimus Lohjanjärven Osuniemenlahdelta ja sen lähiympäristöstä. (M. Sc. thesis). University of Turku, Turku, pp. 1–143.

Heltai, G., Percsich, K., Halász, G., Jung, K., Fekete, I., 2005. Estimation of ecotoxicological potential of contaminated sediments based on sequential extraction procedure with supercritical CO_2 and subcritical H_2O solvents. Microchem. J. 2005, 231–237. https://doi.org/10.1016/j.microc.2004.05.007.

Hietanen, S., Kuparinen, J., 2008. Seasonal and short-term variation in denitrification and anammox at a coastal station on the Gulf of Finland, Baltic Sea. Hydrobiologia 596 (1), 67–77. https://doi.org/10.1007/s10750-007-9058-5.

Hild, E., Brumsack, H.-J., 1998. Major and minor element geochemistry of Lower Aptian sediments from the NW German Basin (core Hohenegglesen KB 40). Cretac. Res. 19 (5), 615–633. https://doi.org/10.1006/cres.1998.0122.

Hoffmann, M., Mikutta, C., Kretzschmar, R., 2012. Bisulfide reaction with natural organic matter enhances arsenite sorption: insights from X-ray absorption spectroscopy. Environmental Science & Technology 46 (21), 11788–11797. https://doi.org/10.1021/es302590x.

Holby, O., Evans, S., 1996. The vertical distribution of Chernobyl-derived radionuclides in a Baltic Sea sediment. J. Environ. Radioact. 33 (2), 129–145. https://doi.org/10.1016/0265-931X(95)00089-S.

Hu, G., Dam-Johansen, K., Wedel, S., Hansen, J.P., 2006. Decomposition and oxidation of pyrite. Prog. Energy Combust. Sci. 32 (3), 295–314. https://doi.org/10.1016/j.pecs.2005.11.004.

Huerta-Diaz, M.A., Morse, J.W., 1992. Pyritization of trace metals in anoxic marine sediments. Geochim. Cosmochim. Acta 56 (7), 2681–2702. https://doi.org/10.1016/0016-7037(92)90353-K.

Huerta-Diaz, M.A., Tessier, A., Carignan, R., 1998. Geochemistry of trace metals associated with reduced sulfur in freshwater sediments. Appl. Geochem. 13 (2), 213–233. https://doi.org/10.1016/S0883-2927(97)00060-7.

Huser, B.J., Köhler, S.J., Wilander, A., Johansson, K., Fölster, J., 2011. Temporal and spatial trends for trace metals in streams and rivers across Sweden (1996–2009). Biogeosciences 8, 1813–1823. https://doi.org/10.5194/bg-8-1813-2011.

Huser, B.J., Fölster, J., Köhler, S.J., 2012. Lead, zinc, and chromium concentrations in acidic headwater streams in Sweden explained by chemical, climatic, and land-use variations. Biogeosciences 9 (11), 4323–4335. https://doi.org/10.5194/bg-9-4323-2012.

Ingri, J., Widerlund, A., Suteerasak, T., Bauer, S., Elming, S.-Å., 2014. Changes in trace metal sedimentation during freshening of a coastal basin. Mar. Chem. 167, 2–12. https://doi.org/10.1016/j.marchem.2014.06.010.

Jeong, C.Y., Young, S.D., Marshall, S.J., 2007. Competitive adsorption of heavy metals in humic substances by s simple ligand model. Soil Sci. Soc. Am. J. 71 (2), 515–528. https://doi.org/10.2136/sssaj2005.0281.

Jilbert, T., Slomp, C.P., 2013. Iron and manganese shuttles control the formation of authigenic phosphorus minerals in the euxinic basins of the Baltic Sea. Geochim. Cosmochim. Acta 107, 155–169. https://doi.org/10.1016/j.gca.2013.01.005.

Jilbert, T., Asmala, E., Schröder, C., Tiihonen, R., Myllykangas, J.-P., Virtasalo, J.J., Kotilainen, A., Peltola, P., Ekholm, P., Hietanen, S., 2018. Impacts of flocculation on the distribution and diagenesis of iron in boreal estuarine sediments. Biogeosciences 15, 1243–1271. https://doi.org/10.5194/bg-15-1243-2018.

Jokinen, S.A., Virtasalo, J.J., Kotilainen, A.T., Saarinen, T., 2015. Varve microfabric record of seasonal sedimentation and bottom flow-modulated mud deposition in the coastal northern Baltic Sea. Mar. Geol. 366, 79–96. https://doi.org/10.1016/j.margeo.2015.05.003.

Jokinen, S.A., Virtasalo, J.J., Jilbert, T., Kaiser, J., Dellwig, O., Arz, H.W., Hänninen, J., Arppe, L., Collander, M., Saarinen, T., 2018. A 1500-year multiproxy record of coastal hypoxia from the northern Baltic Sea indicates unprecedented deoxygenation over the 20th century. Biogeosciences 15, 3975–4001. https://doi.org/10.5194/bg-15-3975-2018.

Jones, B., Turki, A., 1997. Distribution and speciation of heavy metals in surficial sediments from the Tees Estuary, north-east England. Mar. Pollut. Bull. 34 (10), 768–779. https://doi.org/10.1016/S0025-326X(97)00047-7.

Jönsson, A., Lindström, M., Carman, R., Mörth, C.-M., Meili, M., Gustafsson, Ö., 2005. Evaluation of the Stockholm Archipelago sediments, northwestern Baltic Sea Proper, as a trap for freshwater runoff organic carbon. J. Mar. Syst. 56 (1–2), 167–178.

Karbassi, A.R., Nouri, J., Ayaz, G.O., 2007. Flocculation of trace metals during mixing of Talar River water with Caspian Seawater. International Journal of Environmental Research 1 (1), 66–73.

Katko, T., Luonsi, A., Juuti, P.S., 2005. Water pollution and strategies in Finnish pulp and paper industries in the 20th century. Int. J. Environ. Pollut. 23 (4), 368–387. https://doi.org/10.1504/IJEP.2005.007600.

Kersten, M., 2002. Speciation of trace metals in sediments. In: Ure, N.A., Davidson, C.M. (Eds.), Chemical Speciation in the Environment, Second edition Blackwell Science, London, pp. 301–317. https://doi.org/10.1002/9780470988312.ch11.

Kheboian, C., Bauer, C.F., 1987. Accuracy of selective extraction procedures for metal speciation in model aquatic sediments. Anal. Chem. 59 (10), 1417–1423. https://doi.org/10.1021/ac00137a010.

Kim, C., Zhou, Q., Deng, B., Thornton, E.C., Xu, H., 2001. Chromium(VI) reduction by hydrogen sulfide in aqueous media: stoichiometry and kinetics. Environmental Science & Technology 35 (11), 2219–2225. https://doi.org/10.1021/es0017007.

Klaminder, J., Appleby, P., Crook, P., Renberg, I., 2012. Post-deposition diffusion of ^{137}Cs in lake sediment: implications for radiocaesium dating. Sedimentology 59 (7), 2259–2267. https://doi.org/10.1111/j.1365-3091.2012.01343.x.

Koistinen, J., Sjöblom, M., Spilling, K., 2018. Determining inorganic and organic nitrogen. Methods in Molecular Biology. Humana Press, New York, USA, pp. 1–10. https://doi.org/10.1007/7651_2018_128.

Kortelainen, P., Saukkonen, S., Mattsson, T., 1997. Leaching of nitrogen from forested catchments in Finland. Glob. Biogeochem. Cycles 11 (4), 627–638. https://doi.org/10.1029/97GB01961.

Kraal, P., Slomp, C.P., Reed, D.C., Reichart, G.-J., Poulton, S.W., 2012. Sedimentary phosphorus and iron cycling in and below the oxygen minimum zone of the northern Arabian Sea. Biogeosciences 9, 2603–2624. https://doi.org/10.5194/bg-9-2603-2012.

Krupadam, R.J., Sarin, R., Anjaneyulu, Y., 2003. Distribution of trace metals and organic matter in the sediments of Godavari Estuary of Kakinada Bay, East Coast of India. Water Air Soil Pollut. 150 (1–4), 299–318. https://doi.org/10.1023/A:1026132909289.

Lahermo, P., Väänänen, P., Tarvainen, T., Salminen, R., 1996. Geochemical Atlas of Finland Part 3: Environmental Geochemistry – Stream Waters and Sediments. Geological Survey of Finland, Espoo, Finland, pp. 1–150.

Lalonde, K., Mucci, A., Ouellet, A., Gélinas, Y., 2012. Preservation of organic matter in sediments promoted by iron. Nature 483, 198–200. https://doi.org/10.1038/nature10855.

Large, R.R., Danyushevsky, L., Hollit, C., Maslennikov, V., Meffre, S., Gilbert, S., Bull, S., Scott, R., Emsbo, P., Thomas, H., Singh, B., Foster, J., 2009. Gold and trace element zonation in pyrite using a laser imaging technique: implications for the timing of gold in orogenic and Carlin-style sediment-hosted deposits. Econ. Geol. 104 (5), 635–668. https://doi.org/10.2113/gsecongeo.104.5.635.

Large, R.R., Halpin, J.A., Danyushevsky, L.V., Maslennikov, V.V., Bull, S.W., Long, J.A., Gregory, D.D., Lounejeva, E., Lyons, T.W., Sack, P.J., McGoldrick, P.J., Calver, C.R., 2014. Trace element content of sedimentary pyrite as a new proxy for deep-time ocean–atmosphere evolution. Earth Planet. Sci. Lett. 389, 209–220. https://doi.org/10.1016/j.epsl.2013.12.020.

Laudon, H., Hedtjärn, J., Schelker, J., Bishop, K., Sørensen, R., Ågren, A., 2009. Response of dissolved organic carbon following forest harvesting in a boreal forest. Ambio 38 (7), 381–386. https://doi.org/10.1579/0044-7447-38.7.381.

Leenheer, J.A., Brown, G.K., MacCarthy, P., Cabaniss, S.E., 1998. Models of metal binding structures in fulvic acids from the Suwannee River, Georgia. Environmental Science & Technology 32 (16), 2410–2416. https://doi.org/10.1021/es9708979.

Lepistö, A., Futter, M.N., Kortelainen, P., 2014. Almost 50 years of monitoring shows that climate, not forestry, controls long-term organic carbon fluxes in a large boreal watershed. Glob. Chang. Biol. 20 (4), 1225–1237. https://doi.org/10.1111/gcb.12491.

Levshina, S., 2018. An assessment of metal-humus complexes in river waters of the Upper Amur basin, Russia. Environ. Monit. Assess. 190 (1), 18. https://doi.org/10.1007/s10661-017-6384-6.

Lidman, F., Köhler, S.J., Mörth, C.-M., Laudon, H., 2014. Metal transport in the boreal landscape—the role of wetlands and the affinity for organic matter. Environmental Science & Technology 48 (7), 3783–3790. https://doi.org/10.1021/es4045506.

Lidman, F., Boily, Å., Laudon, H., Köhler, S.J., 2017. From soil water to surface water – how the riparian zone controls element transport from a boreal forest to a stream. Biogeosciences 14 (12), 3001–3014. https://doi.org/10.5194/bg-14-3001-2017.

Lion, L.W., Altmann, R.S., Leckie, J.O., 1982. Trace-metal adsorption characteristics of estuarine particulate matter: evaluation of contributions of iron/manganese oxide and organic surface coatings. Environmental Science & Technology 16 (10), 660–666. https://doi.org/10.1021/es00104a007.

Little, S.H., Vance, D., Lyons, T.W., McManus, J., 2015. Controls on trace metal authigenic enrichment in reducing sediments: insights from modern oxygen-deficient settings. Am. J. Sci. 315 (2), 77–119. https://doi.org/10.2475/02.2015.01.

Liu, H., Li, L., Yin, C., Shan, B., 2008. Fraction distribution and risk assessment of heavy metals in sediments of Moshui Lake. J. Environ. Sci. 20, 390–397. https://doi.org/10.1016/S1001-0742(08)62069-0.

Lourino-Cabana, B., Billon, G., Lesven, L., Sabbe, K., Gillan, D.-C., Gao, Y., Leermakers, M., Bayens, W., 2014. Monthly variation of trace metals in North Sea sediments. From experimental data to modeling calculations. Mar. Pollut. Bull. 87 (1–2), 237–246. https://doi.org/10.1016/j.marpolbul.2014.07.053.

Luoma, S.N., 1983. Bioavailability of trace metals to aquatic organisms — a review. Sci. Total Environ. 28, 1–3, 1–22. https://doi.org/10.1016/S0048-9697(83)80004-7.

Luotamo, I., Luotamo, M., 1979. Koverharin rauta- ja terästehtaan vesistövaikutuksista. Loppuraportti: II Sedimentin raskasmetallipitoisuuksista. Tvärminne Zoological Station. University of Helsinki, pp. 1–22.

Mannio, J., Verta, M., Järvinen, O., 1993. Trace metal concentrations in the water of small lakes, Finland. Appl. Geochem. 8 (Supplement 2), 57–59. https://doi.org/10.1016/S0883-2927(09)80011-5.

Mantoura, R.F.C., Dickson, A., Riley, J.P., 1978. The complexation of metals with humic materials in natural waters. Estuar. Coast. Mar. Sci. 6 (4), 387–408. https://doi.org/10.1016/0302-3524(78)90130-5.

Mattsson, T., Kortelainen, P., Räike, A., 2005. Export of DOM from boreal catchments: impacts of land use cover and climate. Biogeochemistry 76 (2), 373–394. https://doi.org/10.1007/s10533-005-6897-x.

McTiernan, K.B., Jarvis, S.C., Scholefield, D., Hayes, M.H.B., 2001. Dissolved organic carbon losses from grazed grasslands under different management regimes. Water Res. 35 (10), 2565–2569. https://doi.org/10.1016/S0043-1354(00)00528-5.

Mehra, O.P., Jackson, M.L., 1958. Iron oxide removal from soils and clays by a dithionite-citrate system buffered with sodium bicarbonate. Clay Clay Miner. 7, 317–327. https://doi.org/10.1346/CCMN.1958.0070122.

Meriläinen, J.J., Kustula, V., Witick, A., Haltia-Hovi, E., Saarinen, T., 2010. Pollution history from 256 BC to AD 2005 inferred from the accumulation of elements in a varve record of Lake Korttajärvi in Finland. J. Paleolimnol. 44 (2), 531–545. https://doi.org/10.1007/s10933-010-9435-3.

Millward, G.E., 1995. Processes affecting trace element speciation in estuaries. Analyst 120 (3), 609–614. https://doi.org/10.1039/AN9952000609.

Morgan, B., Rate, A.W., Burton, E.D., 2012. Trace element reactivity in FeS-rich estuarine sediments: influence of formation environment and acid sulfate soil drainage. Sci. Total Environ. 438, 463–476. https://doi.org/10.1016/j.scitotenv.2012.08.088.

Morse, J.W., Luther III, G.W., 1999. Chemical influences on trace metal-sulfide interactions in anoxic sediments. Geochim. Cosmochim. Acta 63 (19–20), 3373–3378. https://doi.org/10.1016/S0016-7037(99)00258-6.

Müller, A., 2002. Pyritization of iron and trace metals in anoxic fjord sediments (Nordåsvannet fjord, western Norway). Appl. Geochem. 17 (7), 923–933. https://doi.org/10.1016/S0883-2927(01)00130-5.

Neubauer, E., Köhler, S.J., von der Kammer, F., Laudon, H., Hofmann, T., 2013. Effect of pH and stream order on iron and arsenic speciation in boreal catchments. Environmental Science & Technology 47 (13), 7120–7128. https://doi.org/10.1021/es401193j.

Nobi, E.P., Dilipan, E., Thangaradjou, T., Sivakumar, K., Kannan, L., 2010. Geochemical and geo-statistical assessement of heavy metal concentration in the sediments of different coastal ecosystems of Andaman Islands, India. Estuar. Coast. Shelf Sci. 87, 253–264. https://doi.org/10.1016/j.ecss.2009.12.019.

Nriagu, J.O., 1979. Global inventory of natural and anthropogenic emissions of trace metals to the atmosphere. Nature 279, 409–411. https://doi.org/10.1038/279409a0.

Nystrand, M.I., Österholm, P., Nyberg, M.E., Gustafsson, J.P., 2012. Metal speciation in rivers affected by enhanced soil erosion and acidity. Appl. Geochem. 27, 906–916. https://doi.org/10.1016/j.apgeochem.2012.01.009.

Ojala, A.E.K., Luoto, T.P., Virtasalo, J.J., 2017. Establishing a high-resolution surface sediment chronology with multiple dating methods – testing ^{137}Cs determination with Nurmijärvi clastic-biogenic varves. Quat. Geochronol. 37, 32–41. https://doi.org/10.1016/j.quageo.2016.10.005.

Olson, L., Quinn, K.A., Siebecker, M.G., Luther III, G.W., Hastings, D., Morford, J.L., 2017. Trace metal diagenesis in sulfidic sediments: insights from Chesapeake Bay. Chem. Geol. 452, 47–59. https://doi.org/10.1016/j.chemgeo.2017.01.018.

Oni, S.K., Futter, M.N., Bishop, K., Köhler, S.J., Ottosson-Löfvenius, M., Laudon, H., 2013. Long-term patterns in dissolved organic carbon, major elements and trace metals in boreal headwater catchments: trends, mechanisms and heterogeneity. Biogeosciences 10, 2315–2330. https://doi.org/10.5194/bg-10-2315-2013.

Oueslati, W., Helali, M.A., Noureddine, Z., Sebei, A., Added, A., Aleya, L., 2018. Sulfide influence on metal behavior in a polluted southern Mediterranean lagoon: implications for management. Environ. Sci. Pollut. Res. 23 (3), 2248–2264. https://doi.org/10.1007/s11356-017-0529-6.

Pacyna, J.M., Scholtz, T., Li, Y.-F.A., 2005. Global budget of trace metal sources. Environ. Rev. 3 (2), 145–159. https://doi.org/10.1139/a95-006.

Pan, K., Wang, W.-X., 2012. Trace metal contamination in estuarine and coastal environments in China. Sci. Total Environ. 421–422, 3–16. https://doi.org/10.1016/j.scitotenv.2011.03.013.

Parker, J.C., Rae, J.E., 1998. Environmental Interactions of Clays: Clays and the Environment. Springer Verlag, Berlin Heidelberg New York, p. 271.

Passos, E.A., Alves, J.C., dos Santos, I.S., Alves, J.P.H., Garcia, C.A.B., Spinola Costa, A.C., 2010. Assessment of trace metals contamination in estuarine sediments using a sequential extraction technique and principal component analysis. Microchem. J. 96, 50–57. https://doi.org/10.1016/j.microc.2010.01.018.

Pejman, A., Bidhendi, G.N., Ardestani, M., Saeedi, M., Baghvand, A., 2017. Fractionation of heavy metals in sediments and assessment of their availability risk: a case study in the northwestern of Persian Gulf. Mar. Pollut. Bull. 114 (2), 881–887. https://doi.org/10.1016/j.marpolbul.2016.11.021.

Pickering, W.F., 1986. Metal ion speciation — soils and sediments (a review). Ore Geol. Rev. 1 (1), 83–146. https://doi.org/10.1016/0169-1368(86)90006-5.

Pokrovsky, O.S., Schott, J., 2002. Iron colloids/organic matter associated transport of major and trace elements in small boreal rivers and their estuaries (NW Russia). Chem. Geol. 190, 141–179. https://doi.org/10.1016/S0009-2541(02)00115-8.

Poulton, S.W., Canfield, D.E., 2005. Development of a sequential extraction procedure for iron: implications for iron partitioning in continentally derived particulates. Chem. Geol. 214 (3–4), 209–221. https://doi.org/10.1016/j.chemgeo.2004.09.003.

Prajith, A., Rao, V.P., Chakrabotry, P., 2016. Distribution, provenance and early diagenesis of major and trace metals in sediment cores from the Mandovi estuary, western India. Estuar. Coast. Shelf Sci. 170, 173–185. https://doi.org/10.1016/j.ecss.2016.01.014.

Premier, V., Machado, A.A.S., Mitchell, S., Zarfl, C., Spencer, K., Toffolon, M., 2019. A model-based analysis of metal fate in Thames Estuary. Estuar. Coasts 32 (4), 1185–1201. https://doi.org/10.1007/s12237-019-00544-y.

R Core Team, 2017. R: A Language and Environment for Statistical Computing. R Foundation for Statistical Computing, Vienna, Austria https://www.R-project.org/.

Rainbow, P.S., 2007. Trace metal bioaccumulation: models, metabolic availability and toxicity. Environ. Int. 33, 576–582. https://doi.org/10.1016/j.envint.2006.05.007.

Rainbow, P.S., Luoma, S.N., 2011. Metal toxicity, uptake and bioaccumulation in aquatic invertebrates — modelling zinc in crustaceans. Aquat. Toxicol. 105, 455–465. https://doi.org/10.1016/j.aquatox.2011.08.001.

Raiswell, R., 2011. Iron transport from the continents to the open ocean: the aging-rejuvenation cycle. Elements 7 (2), 101–106. https://doi.org/10.2113/gselements.7.2.101.

Raiswell, R., Canfield, D.E., Berner, R.A., 1994. A comparison of iron extraction methods for the determination of degree of pyritisation and the recognition of iron-limited pyrite formation. Chem. Geol. 111 (1–4), 101–110. https://doi.org/10.1016/0009-2541(94)90084-1.

Reese, B.K., Finneran, D.W., Mills, H.J., Zhu, M., Morse, J.W., 2011. Examination and refinement of the determination of aqueous hydrogen sulfide by the methylene blue method. Aquat. Geochem. 17, 567–582. https://doi.org/10.1007/s10498-011-9128-1.

Reimann, C., Filzmoser, P., Garrett, R.G., Dutter, R., 2008. Statistical Data Analysis Explained: Applied Environmental Statistics with R. John Wiley & Sons Ltd, West Sussex, England, pp. 1–362.

Reuter, J.H., Perdue, E.M., 1977. Importance of heavy metal-organic matter interactions in natural waters. Geochim. Cosmochim. Acta 41 (2), 325–334. https://doi.org/10.1016/0016-7037(77)90240-X.

Richir, J., Gobert, S., 2016. Trace elements in marine environments: occurrence, threats and monitoring with special focus on the coastal Mediterranean. Environmental & Analytical Toxicology 6 (1), 1000349. https://doi.org/10.4172/2161-0525.1000349.

Rigaud, S., Radakovitch, O., Couture, R.-M., Deflandre, B., Cossa, D., Garnier, C., Garnier, J.-M., 2013. Mobility and fluxes of trace elements and nutrients at the sediment–water interface of a lagoon under contrasting water column oxygenation conditions. Appl. Geochem. 32, 35–51. https://doi.org/10.1016/j.apgeochem.2012.12.003.

Roos, M., Åström, M., 2005. Hydrogeochemistry of rivers in an acid sulphate soil hotspot area in western Finland. Agric. Food Sci. 14, 24–33. https://doi.org/10.2137/1459606054224075.

Rosenthal, Y., Lam, P., Boyle, E.A., Thomson, J., 1995. Authigenic cadmium enrichments in suboxic sediments: precipitation and postdepositional mobility. Earth Planet. Sci. Lett. 132 (1–4), 99–111. https://doi.org/10.1016/0012-821X(95)00056-I.

Rühling, Å., Tyler, G., 2001. Changes in atmospheric deposition rates of heavy metals in Sweden a summary of Nationwide Swedish surveys in 1968/70–1995. Water, Air, and Soil Pollution: Focus 1 (3–4), 311–323. https://doi.org/10.1023/A:1017584928458.

Ruttenberg, K.C., 1992. Development of a sequential extraction method for different forms of phosphorus in marine sediments. Limnol. Oceanogr. 37 (7), 1460–1482. https://doi.org/10.4319/lo.1992.37.7.1460.

Salomons, W., Förstner, U., 1980. Trace metal analysis on polluted sediments. Part II: evaluation of environmental impact. Environ. Technol. 1, 506–517.

Samani, A.R.V., Karbassi, A.R., Fakhraee, M., Heidari, M., Vaezi, A.R., Valikhani, Z., 2014. Effect of dissolved organic carbon and salinity on flocculation process of heavy metals during mixing of the Navrud River water with Caspian Seawater. Desalin. Water Treat. 55 (4), 926–934. https://doi.org/10.1080/19443994.2014.920730.

Santos-Echeandia, J., Prego, R., Cobelo-García, A., Millward, G.E., 2009. Porewater geochemistry in a Galician Ria (NW Iberian Peninsula): implications for benthic fluxes of dissolved trace elements (Co, Cu, Ni, Pb, V, Zn). Mar. Chem. 117 (1–4), 77–87. https://doi.org/10.1016/j.marchem.2009.05.001.

Santschi, P.H., Lenhart, J.J., Honeyman, B.D., 1997. Heterogeneous processes affecting trace contaminant distribution in estuaries: the role of natural organic matter. Mar. Chem. 58 (1–2), 99–125. https://doi.org/10.1016/S0304-4203(97)00029-7.

Sarmiento, J.L., Gruber, N., 2006. Ocean Biogeochemical Dynamics. Princeton University Press, Princeton, NJ, pp. 1–503.

Savage, C., Leavitt, P.R., Elmgren, R., 2010. Effects of land use, urbanization, and climate variability on coastal eutrophication in the Baltic Sea. Limnol. Oceanogr. 55 (3), 1033–1046. https://doi.org/10.4319/lo.2010.55.3.1033.

Sawicka, J.E., Brüchert, V., 2017. Annual variability and regulation of methane and sulfate fluxes in Baltic Sea estuarine sediments. Biogeosciences 14, 325–339. https://doi.org/10.5194/bg-14-325-2017.

Schelker, J., Eklöf, K., Bishop, K., Laudon, H., 2012. Effects of forestry operations on dissolved organic carbon concentrations and export in boreal first-order streams. Journal of Geophysical Research: Biogeosciences 117 (G1), G01011. https://doi.org/10.1029/2011JG001827.

Schintu, M., Marrucci, A., Marras, B., Galgani, F., Buosi, C., Ibba, A., Cherchi, A., 2016. Heavy metal accumulation in surface sediments at the port of Cagliari (Sardinia, western Mediterranean): environmental assessment using sequential extractions and benthic foraminifera. Mar. Pollut. Bull. 111 (1–2), 45–56. https://doi.org/10.1016/j.marpolbul.2016.07.029.

Schnitzer, M., Kerndorf, H., 1981. Reactions of fulvic acid with metal ions. Water Air Soil Pollut. 15 (1), 97–108. https://doi.org/10.1007/BF00285536.

Scholz, F., Neumann, T., 2007. Trace element diagenesis in pyrite-rich sediments of the Achterwasser lagoon, SW Baltic Sea. Mar. Chem. 107 (4), 516–532. https://doi.org/10.1016/j.marchem.2007.08.005.

Schoonen, M.A.A., 2004. Mechanisms of sedimentary pyrite formation. In: Amend, J.P., Edwards, K.J., Lyons, T.W. (Eds.), Sulfur Biogeochemistry—Past and Present. Geological Society of America, Special Paper vol. 379, pp. 117–134.

Schöpp, W., Posch, M., Mylona, S., Johansson, M., 2003. Long-term development of acid deposition (1880–2030) in sensitive freshwater regions in Europe. Hydrol. Earth Syst. Sci. 7 (4), 436–446. https://doi.org/10.5194/hess-7-436-2003.

Schultz, M.F., Benjamin, M.M., Ferguson, J.F., 1987. Adsorption and desorption of metals on ferrihydrite: reversibility of the reaction and sorption properties of the regenerated solid. Environmental Science & Technology 21 (9), 863–869. https://doi.org/10.1021/es00163a003.

Shaw, T.J., Gieskes, J.M., Jahnke, R.A., 1990. Early diagenesis in differing depositional environments: the response of transition metals in pore water. Geochim. Cosmochim. Acta 54 (5), 1233–1246. https://doi.org/10.1016/0016-7037(90)90149-F.

Sholkovitz, E.R., 1978. The flocculation of dissolved Fe, Mn, Al, Cu, Ni, Co and Cd during estuarine mixing. Earth Planet. Sci. Lett. 41, 77–86. https://doi.org/10.1016/0012-821X(78)90043-2.

Sholkovitz, E.R., Boyle, E.A., Price, N.B., 1978. The removal of dissolved humic acids and iron during estuarine mixing. Earth Planet. Sci. Lett. 40, 130–136. https://doi.org/10.1016/0012-821X(78)90082-1.

Silburn, B., Kröger, S., Parker, E.R., Sivyer, D.B., Hicks, N., Powell, C.F., Johnson, M., Greenwood, N., 2017. Benthic pH gradients across a range of shelf sea sediment types linked to sediment characteristics and seasonal variability. Biogeochemistry 135 (1–2), 69–88. https://doi.org/10.1007/s10533-017-0323-z.

Singh, S.K., Subramanian, V., 1984. Hydrous Fe and Mn oxides – scavengers of heavy metals in the aquatic environment. Crit. Rev. Environ. Control. 14 (1), 33–90. https://doi.org/10.1080/10643388409381713.

Skjelkvåle, B.L., Andersen, T., Fjeld, E., Mannio, J., Wilander, A., Johansson, K., Jensen, J.P., Moiseenko, T., 2001. Heavy metal surveys in Nordic lakes; concentrations, geographic patterns and relation to critical limits. Ambio 30 (1), 2–10. https://doi.org/10.1579/0044-7447-30.1.2.

Sternbeck, J., Sohlenius, G., Hallberg, R.O., 2000. Sedimentary trace elements as proxies to depositional changes induced by a Holocene fresh-brackish water transition. Aquat. Geochem. 6 (3), 325–345. https://doi.org/10.1023/A:1009680714930.

Stipa, T., 1999. Water exchange and mixing in a semi-enclosed coastal basin (Pohja Bay). Boreal Environ. Res. 4, 307–317.

Stolpe, B., Hassellöv, M., 2007. Changes in size distribution of fresh water nanoscale colloidal matter and associated elements on mixing with seawater. Geochim. Cosmochim. Acta 71 (13), 3292–3301. https://doi.org/10.1016/j.gca.2007.04.025.

Stolpe, B., Guo, L., Shiller, A.M., Aiken, G.R., 2013. Abundance, size distributions and trace-element binding of organic and iron-rich nanocolloids in Alaskan rivers, as revealed by field-flow fractionation and ICP-MS. Geochim. Cosmochim. Acta 105, 221–239. https://doi.org/10.1016/j.gca.2012.11.018.

Sunda, W.G., Lewis, J.A.M., 1978. Effect of complexation by natural organic ligands on the toxicity of copper to unicellular alga, *Monochrysis lutheri*. Limnol. Oceanogr. 23 (5), 870–876. https://doi.org/10.4319/lo.1978.23.5.0870.

Sundaray, S.K., Nayak, B.B., Lin, S., Bhatta, D., 2011. Geochemical speciation and risk assessment of heavy metals in the river estuarine sediments — a case study: Mahanadi basin, India. J. Hazard. Mater. 186, 1837–1846. https://doi.org/10.1016/j.jhazmat.2010.12.081.

Tankere-Muller, S., Zhang, H., Davison, W., Finke, N., Larsen, O., Stahl, H., Glud, R.N., 2007. Fine scale remobilisation of Fe, Mn, Co, Ni, Cu and Cd in contaminated marine sediment. Mar. Chem. 106 (1–2), 192–207. https://doi.org/10.1016/j.marchem.2006.04.005.

Tessier, A., Campbell, P.G.C., Bisson, M., 1979. Sequential extraction procedure for the speciation of particulate trace metals. Anal. Chem. 51 (7), 844–851. https://doi.org/10.1021/ac50043a017.

Tipping, E., Lofts, S., Lawlor, A.J., 1998. Modelling the chemical speciation of trace metals in the surface waters of the Humber system. Sci. Total Environ. 210–211, 63–77. https://doi.org/10.1016/S0048-9697(98)00045-X.

Turner, A., Martino, M., Le Roux, S.M., 2002. Trace metal distribution coefficients in the Mersey Estuary, UK: evidence for salting out of metal complexes. Environmental Science & Technology 36 (21), 4578–4584. https://doi.org/10.1021/es020075y.

Tüzen, M., 2003. Determination of trace metals in the River Yeşilırmak sediments in Tokat, Turkey using sequential extraction procedure. Microchem. J. 74 (1), 105–110. https://doi.org/10.1016/S0026-265X(02)00174-1.

Vallius, H., 2009. Heavy metal distribution in the modern soft surface sediments off the Finnish coast of the Gulf of Finland. Baltica 22, 65–76.

Van der Veer, G., 2006. Geochemical soil survey of The Netherlands. Atlas of major and trace elements in topsoil and parent material; assessment of natural and anthropogenic enrichment factors. Neth. Geogr. Stud. 347, 1–245. http://igitur-archive.library.uu.nl/dissertations/2006-1011-200742/full.pdf, Accessed date: 1 January 2020.

Verta, M., Tolonen, J., Simola, H., 1989. History of heavy metal pollution in Finland as recorded by lake sediments. Sci. Total Environ. 87–88, 1–18. https://doi.org/10.1016/0048-9697(89)90222-2.

Virtasalo, J.J., Kohonen, T., Vuorinen, I., Huttula, T., 2005. Sea bottom anoxia in the Archipleago Sea, northern Baltic Sea – implications for phosphorus remineralization at the sediment surface. Mar. Geol. 224, 103–122. https://doi.org/10.1016/j.margeo.2005.07.010.

Virtasalo, J.J., Hämäläinen, J., Kotilainen, A.T., 2014a. Toward a standard stratigraphical classification practice for the Baltic Sea sediments: the CUAL approach. Boreas 43 (4), 924–938. https://doi.org/10.1111/bor.12076.

Virtasalo, J.J., Ryabchuk, D., Kotilainen, A.T., Zhamoida, V., Grigoriev, A., Sivkov, V., Dorokhova, E., 2014b. Midlle Holocene to present sedimentary environment in the easternmost Gulf of Finland (Baltic Sea) and the birth of the Neva River. Mar. Geol. 350, 84–96. https://doi.org/10.1016/j.margeo.2014.02.003.

Virtasalo, J.J., Schröder, J.F., Luoma, S., Majaniemi, J., Mursu, J., Scholten, J., 2019. Submarine groundwater discharge site in the First Salpausselkä ice-marginal formation. Solid Earth 10, 405–423. https://doi.org/10.5194/se-10-405-2019.

Wallmann, K., Kersten, M., Gruber, J., Förstner, U., 1992. Artifacts in the determination of trace metal binding forms in anoxic sediments by sequential extraction. Int. J. Environ. Anal. Chem. 51 (1–4), 187–200. https://doi.org/10.1080/03067319308027624.

Wällstedt, T., Björkvald, L., Gustafsson, J.P., 2010. Increasing concentrations of arsenic and vanadium in (southern) Swedish streams. Appl. Geochem. 25, 1162–1175. https://doi.org/10.1016/j.apgeochem.2010.05.002.

Wang, F., Tessier, A., 2009. Zero-valent sulfur and metal speciation in sediment porewaters of freshwater lakes. Environmental Science & Technology 43 (19), 7252–7257. https://doi.org/10.1021/es8034973.

Wang, W., Chen, M., Guo, L., WAng, W.-X., 2017. Size partitioning and mixing behavior of trace metals and dissolved organic matter in a South China estuary. Sci. Total Environ. 603–604, 434–444. https://doi.org/10.1016/j.scitotenv.2017.06.121.

Warren, L.A., Haack, E.A., 2001. Biogeochemical controls on metal behaviour in freshwater environments. Earth Sci. Rev. 54, 261–320. https://doi.org/10.1016/S0012-8252(01)00032-0.

Wassermann, J.C., Oliveira, F.B.L., Bidarra, M., 1998. Cu and Fe associated with humic acids in sediments of a tropical coastal lagoon. Org. Geochem. 28 (12), 813–822. https://doi.org/10.1016/S0146-6380(98)00044-8.

Wei, B., Yang, L., 2010. A review of heavy metal contaminations in urban soils, urban road dusts and agricultural soils from China. Microchem. J. 94, 99–107. https://doi.org/10.1016/j.microc.2009.09.014.

Weliky, K., Suess, E., Ungerer, C.A., Muller, P.J., Fischer, K., 1983. Problems with accurate carbon measurements in marine sediments and particulate matter in seawater: a new approach. Limnol. Oceanogr. 28 (6), 1252–1259. https://doi.org/10.4319/lo.1983.28.6.1252.

Wells, M.L., Smith, G.J., Bruland, K.W., 2000. The distribution of colloidal and particulate bioactive metals in Narragansett Bay, RI. Mar. Chem. 71, 143–163. https://doi.org/10.1016/S0304-4203(00)00046-3.

Weng, L., Temminghoff, E.J.M., Lofts, S., Tipping, E., van Riemsdijk, W.H., 2002. Complexation with dissolved organic matter and solubility control of heavy metals in a sandy soil. Environmental Science & Technology 36 (2), 4804–4810. https://doi.org/10.1021/es0200084.

Winterhalter, B., Flodén, T., Ignatius, H., Axberg, S., Niemistö, L., 1981. Geology of the Baltic Sea. In: Voipio, A. (Ed.), The Baltic Sea. Elsevier, Amsterdam, the Netherlands, pp. 1–121.

Yang, R., van der Berg, C.M.G., 2009. Metal complexation by humic substances in seawater. Environmental Science & Technology 43, 7192–7197. https://doi.org/10.1021/es900173w.

Yi, Y., Yang, Z., Zhang, S., 2011. Ecological risk assessment of heavy metals in sediment and human health assessment of heavy metals in fishes in the middle and lower reaches of the Yangtze River basin. Environ. Pollut. 159, 2575–2585. https://doi.org/10.1016/j.envpol.2011.06.011.

Yu, Y., Song, J., Duan, L., Li, X., Yuan, H., Li, N., 2014. Sedimentary trace-element records of natural and human-induced environmental changes in the East China Sea. J. Paleolimnol. 52 (4), 277–292. https://doi.org/10.1007/s10933-014-9793-3.

Yu, C., Virtasalo, J.J., Karlsson, T., Peltola, P., Österholm, P., Burton, E.D., Arppe, L., Hogmalm, J.K., Ojala, A.E.K., Åström, M., 2015. Iron behavior in a northern estuary: large pools of non-sulfidized Fe(II) associated with organic matter. Chem. Geol. 413, 73–85. https://doi.org/10.1016/j.chemgeo.2015.08.013.

Yu, C., Virtasalo, J.J., Österholm, P., Burton, E.D., Peltola, P., Ojala, A.E.K., Hogmalm, J.K., Åström, M.E., 2016. Manganese accumulation and solid-phase speciation in a 3.5 m thick mud sequence from the estuary of an acidic and Mn-rich creek, northern Baltic Sea. Chem. Geol. 437, 56–66. https://doi.org/10.1016/j.chemgeo.2016.05.016.

Yuan, C., Shi, J., He, B., Liu, J., Liang, L., Jiang, G., 2004. Speciation of heavy metals in marine sediments from the East China Sea by ICP-MS with sequential extraction. Environ. Int. 30 (6), 769–783. https://doi.org/10.1016/j.envint.2004.01.001.

Zonneveld, K.A.F., Versteegh, G.J.M., Kasten, S., Eglinton, T.I., Emeis, K.-C., Huguet, C., Koch, B.P., de Lange, G.J., de Leeuw, J.W., Middelburg, J.J., Mollenhauer, G., Prahl, F.G., Rethemeyer, J., Wakeham, S.G., 2010. Selective preservation of organic matter in marine environments; processes and impact on the sedimentary record. Biogeosciences 7, 483–511. https://doi.org/10.5194/bg-7-483-2010.